Supporting Information for

Predicting Fluid Flow Regime, Permeability, and Diffusivity in Mudrocks from Multiscale Pore Characterisation

Amirsaman Rezaeyan[1*], Vitaliy Pipich[2], Jingsheng Ma[3], Leon Leu[4], Timo Seemann[5], Gernot Rother[6], Lester C. Barnsley[2,7], and Andreas Busch[1]

[1] Lyell Centre, Institute of GeoEnergy Engineering, Heriot-Watt University, Edinburgh, EH14 4AS, UK

[2] Forschungszentrum Jülich GmbH, Jülich Centre for Neutron Science JCNS at Heinz Maier-Leibnitz Zentrum MLZ, Garching, 85748, Germany

[3] Institute of GeoEnergy Engineering, Heriot-Watt University, Edinburgh, EH14 4AS, UK

[4] Department of Earth Science and Engineering, Imperial College London, London, SW7 2AZ, UK

[5] Clay and Interface Mineralogy, RWTH Aachen University, Aachen, 52072, Germany

[6] Chemical Sciences Division, Oak Ridge National Laboratory, Oak Ridge, TN, 37922, USA

[7] Australian Synchrotron, ANSTO, Clayton, 3168, Australia

*Corresponding author: Amirsaman Rezaeyan (ar104@hw.ac.uk; amirsaman.rezaeyan@gmail.com)

Contents of this file

36 pages, 3 Figures, 7 Tables

Additional Supplementary Materials (Files uploaded separately)

Tables S1 to S7 are the same tables in this file, however, they are provided in *.xlsx.

Introduction

This supporting information provides full details of samples, details of the mineralogical and geochemical compositions of the mudrocks, details of the measurements, full experimental and analytical information, and a detailed description of the results.

S1. Materials

S1.1. Organic Lean Mudrock Samples

The **Opalinus Clay** formation consists of monotonous sequences of shaly, sandy, and carbonate-rich sandy facies at the Mont Terri, St. Ursanne, Switzerland. These samples were obtained from a 4 m core section of the shaly facies of the Opalinus Clay formation at a depth of approximately 230 m at the Mont Terri underground rock laboratory (Busch et al. 2017). The Opalinus Clay was deposited in the Aalenian (Dogger-α, ca. 174 Ma) in a shallow marine setting of an epicontinental sea at water depths of around 10–30 m. The sample set is high in clay content, containing mainly illite and kaolinite, and low in quartz and carbonates (Bossart and Thury 2008).

The **Boom Clay** samples were recovered from a depth of 168 to 246 m in the ON-Mol1 borehole, drilled in 1997, near Mol, Belgium (Jacops et al. 2017a). Based on the lithological variations in Boom Clay, it has been subdivided in four members: the Boeretang Member, the Putte Member, the Terhagen Member, and the Belsele-Waas Member. Samples used in this study originate from the Putte and Boeretang Members and are classified as clayey and silty, respectively. The mineralogy is dominated by illite/smectite and quartz, with minor fractions of muscovite, kaolinite, and K-feldspar (Vandenberghe et al. 2014, Zeelmaekers et al. 2015).

The **Våle Shale** samples were obtained from the Våle formation in the Møre Basin, Norway. Kaolinite, mica/illite and calcite contents are rather small, whereas smectite and quartz are dominant. Mineralogical and elemental composition of sediments indicate a significant change across the Cretaceous–Tertiary boundary. This change is mainly observed between greenish-grey, strongly bioturbated claystones and mudstones of Maastrichtian age and dark grey, less strongly bioturbated mudstones of early Danian age (Gjelberg et al. 2005), with the latter being used in this study.

The **Carmel Claystone** core was taken from a scientific drilling campaign near Green River, Utah, at a burial depth of ~200 m. The Carmel Formation is a 50 m-thick sequence of complex, laterally gradational lithofacies, comprising interbedded red and grey shale and gypsum, red and grey mudstone/siltstone, and fine grained sandstone. The section analysed is high in clay content, containing mainly illite, with lower amounts of quartz and carbonates (Kampman et al. 2016, Kampman et al. 2014). These are interpreted as Mid-Jurassic marine sediments deposited in quiet, subtidal conditions under the influence of periodic hypersaline water and form a regional seal (Blakey et al. 1996).

The **Entrada Siltstone** is directly overlying the Carmel formation. These are alternating aeolian siltstone/sandstone layers of upper Jurassic age. Regionally, the detrital mineralogy of dune facies sandstones comprises subangular to rounded grains of quartz and coating illite around quartz. All samples vary considerably in type and amount of cement, mainly including quartz, dolomite and illite (Kampman 2011).

S1.2. Organic Rich Mudrock Samples

Toarcian (Lias Epsilon) **Posidonia Shale** samples were obtained from the Hills Syncline in northern Germany. The organic matter has been classified as kerogen Type II (Bernard et al. 2012). The shale intervals cored represent a wide range of maturities from premature to overmature that attribute to either Late Cretaceous magmatic heating or deep burial during the Late Jurassic and Early Cretaceous. Deposited in shallow marine environment with upper facies of calcareous shale and lower facies of marlstone, the samples have nearly similar mineralogy and TOCs (Klaver et al. 2012).

Carboniferous Shales have been sampled from the Westphalian C section of the Campine Basin in Belgium, which were taken from well KB186. The samples studied were cored from the depth of 1185-1197 m. These samples contain kerogen type III with slight differences in thermal maturation (Vandewijngaerde et al. 2016).

Upper Jurassic **Haynesville** and upper Jurassic to lower Cretaceous **Bossier** shales of the northwestern Gulf of Mexico Basin are marine transgressive to highstand mudrocks within alternated carbonate-clastic depositional systems (Hammes and Frébourg 2012). Bossier shale samples were obtained from a depth of 3650-3750 m in West Louisiana, USA. The samples have different mineralogy and maturity, but limited TOCs over the ~100 m depth range. The Haynesville samples were obtained from different wells drilled at different intervals of the formation in East Texas. Haynesville strata were buried to over 4000 m and contain various lithology from silty argillaceous to silty calcareous mudstones (Klaver et al. 2015).

The **Eagle Ford** Shale is of late Cretaceous (Cenomanian- to Turonian) age and obtained from East Texas Basin, USA. It is a self-contained petroleum system including several units, interstratified source, seal, and oil- and gas-prone reservoir rocks. These strata diversify significantly within the context of lithofacies, which consist of finely interstratified argillaceous, siltstone and carbonate microfacies. Interstratified with siliciclastic and bioclastic sandstones and siltstones, these multifacies were buried in marine depositional setting (Dawson and Almon 2010). The samples are made of silt-rich aggregation taken from 2500 metre depth and the TOCs range around 3.5 wt. %.

The **Jordan Shale** samples were taken from a black shale formation in Jordan. The oil-bearing kerogen type II strata consists of dark argillaceous silt layers interbedded with sandy claystone. The sea level fluctuations have suggested several facies associations assigned to the fluvial marine depositional environment during Early Cretaceous (from the Barremian to Albian) (Amireh 1997).

Finally, the **Newark Shale** samples originate from the Newark basin in NE USA, deposited in an enormous rifting basin (~8000 km long). The depositional environment is of continental, largely lacustrine origin that ranges from early Triassic (Carnian) to Early Jurassic (Hettangian) age (Olsen et al. 1996). For this study, a lacustrine mudstone sample was selected from a core section of the Newark Basin Coring Project, sampled from the Carnian Lockatong formation in New Jersey. It has a TOC of 2.3 % and is overmature with VR_r = 2.17 % at the depth of 3230 m (Fink et al. 2018).

S2. Experimental and Analytical Methods

S2.1. Quantitative X-Ray Diffraction Analysis

Error! Reference source not found. tabulates a summary of the mineralogical and geochemical properties of the mudrocks studied. X-ray diffraction (XRD) measurements were performed on a Bruker D8 diffractometer using CuKα-radiation produced at 40 kV and 40 mA at RWTH Aachen University, Germany. The diffracted beam was measured with a scintillation detector. Counting time was 3 sec (20 sec for Carmel and Entrada) per step of 0.02° 2θ. Diffractograms were recorded from 2° to 92° 2θ. Rock samples are crushed manually in a mortar with care taken to avoid strain damage and crushed material together with an internal standard (Corundum, 20 wt%) is milled in ethanol with a McCrone Micronising mill (15 min). Quantitative phase analysis was performed by Rietveld refinement using the BGMN-Profex software (Doebelin and Kleeberg 2015) with customised clay mineral structure models (Ufer et al. 2008). The precision of these measurements, from repetitions on the same sample, is better than 1 wt% absolute for phases for which the content is above 2 wt%. Accuracy cannot be determined because of the lack of pure (clay) mineral standards, it is however estimated to be better than 10% (relative). Mineral compositions relate to the crystalline content of the analysed samples. Well-detailed description on the methods has been published previously (Busch et al. 2017, Klaver et al. 2015, Klaver et al. 2012, Fink et al. 2018).The mineralogy of Boom samples was obtained from Jacops et al. (2017b). Mineralogy was determined by Xray diffraction (XRD) analyses as described by Zeelmaekers et al. (2015).

S2.2. Total Organic Carbon Content and Vitrinite Reflectance

TOC content data were measured on powdered samples with a LECO RC-412 Multiphase Carbon/Hydrogen/Moisture Determinator. This instrument operates in a non-isothermal mode with continuous recording of the CO_2 release during oxidation to determine both inorganic and organic carbon contents individually in a single analytical run. Therefore, there is no need to remove carbonates by acid treatment for TOC content measurement. The technique is based on the different decomposition of the phases during heating (Busch et al. 2017). Details of the analytical procedure and instrumentation of vitrinite reflectance measurements are described in Littke et al. (2012).

Table S 1. Mineralogical and geochemical information of all mudrocks.

Sample	Quartz	Albite	K-feldspar	Kaolinite	Illite/Mus/I-S	Montmorillonite	Chlorite	Calcite	Dolomite	Siderite	Hematite	Pyrite
	wt.%	wt.%	wt.%	wt.%	wt.%	wt.%	wt.%	wt.%	wt.%	wt.%	wt.%	wt.%
Opalinus Clay												
CCP01	19.4	1.9	2.2	21.3	40.8	2.5	3.1	3.5	0.8	1.1	0.0	0.7
CCP04	16.0	1.8	2.3	20.9	40.1	3.5	7.9	2.9	0.5	0.8	0.0	0.8
CCP05	16.3	1.4	2.0	22.9	42.4	3.5	3.7	2.9	0.6	1.2	0.0	0.8
CCP06	15.1	1.4	2.3	20.0	46.3	3.5	3.8	2.5	0.5	1.3	0.0	0.7
CCP07	12.3	1.1	1.6	21.9	46.7	3.5	4.0	4.5	0.3	0.5	0.0	0.7
CCP09	12.2	1.7	2.1	20.9	43.0	3.5	6.5	4.5	0.3	0.9	0.0	1.0
CCP10	12.6	1.6	2.5	21.9	41.0	3.5	4.3	7.1	0.3	1.1	0.0	1.2
CCP12	11.5	0.8	1.6	20.2	48.4	3.5	3.9	5.2	0.3	0.5	0.0	1.5
CCP14	12.0	0.8	1.6	21.0	48.5	3.5	4.3	3.4	0.4	0.3	0.0	1.7
Boom Clay												
BC-K4	28.0	1.0	5.0	9.2	29.1	17.9	4.9	2.0	0.0	0.0	0.0	2.0
BC-K10	32.0	2.0	10.0	6.4	22.7	19.7	4.2	0.8	0.6	0.0	0.0	1.0
BC-K11	33.0	3.0	6.0	6.1	23.4	21.7	3.9	0.4	0.5	0.0	0.0	1.0
BC-K2	32.0	3.0	8.0	9.0	26.5	13.8	3.7	0.2	0.0	0.0	0.0	2.0
BC-K9	26.0	0.7	5.0	12.4	26.0	24.0	2.6	0.0	0.0	0.0	0.0	2.0
Vale Shale												
VS1	26.8	2.5	2.0	0.4	14.7	31.2	2.3	17.5	0.0	0.1	0.0	1.8
VS2	20.6	3.1	1.6	0.2	20.0	42.5	2.5	6.9	0.0	0.0	0.0	1.9
VS3	22.6	3.7	2.6	4.6	18.2	35.8	2.2	7.1	0.0	0.1	0.0	2.2
Carmel Claystone												
NPS069	8.1	0.0	3.5	0.0	82.0	0.0	0.0	0.0	2.9	0.0	0.0	3.8
NPS073	5.2	0.0	2.8	0.0	85.7	0.0	0.0	0.0	5.3	0.0	0.0	0.0
NPS077	6.0	0.0	3.2	0.0	79.4	0.0	0.0	0.0	8.5	0.1	0.0	1.8
NPS080	6.1	0.0	3.1	0.0	80.7	0.0	0.0	0.0	7.7	0.1	0.3	2.0
NPS083	5.8	0.0	3.2	0.0	81.1	0.0	0.0	0.0	7.7	0.0	0.0	1.8
NPS086	6.3	0.0	2.3	0.0	79.6	0.0	0.0	0.0	7.0	0.1	3.5	0.6
NPS089	5.5	0.0	2.7	0.0	79.2	0.0	0.0	0.0	7.3	0.1	4.1	0.6
NPS095	4.8	0.0	3.3	0.0	79.9	0.0	0.0	0.0	7.0	0.1	3.8	0.6
Big Hole Carmel												
BH2CC16b	37.2	0.5	12.5	0.0	22.6	0.0	0.0	0.0	26.8	0.0	0.0	0.0
Entrada Siltstone												
EPS1004	43.4	1.5	10.1	0.0	31.9	0.0	0.0	0.1	11.7	0.0	0.0	0.3
EPS3049	41.3	1.6	9.2	0.0	37.2	0.0	0.0	0.2	9.2	0.0	0.2	0.4
EPS3057	37.9	1.6	7.9	0.0	39.4	0.0	0.0	0.1	11.4	0.0	1.1	0.3
EPS3058	43.4	1.5	10.1	0.0	31.9	0.0	0.0	0.1	11.7	0.0	0.0	0.3

EPS3059	44.1	1.7	9.2	0.0	33.9	0.0	0.0	0.2	10.0	0.0	0.2	0.3
EPS3061	35.8	1.4	6.7	0.0	41.0	0.0	0.0	0.2	13.4	0.0	0.2	0.4
EPS3062	36.7	1.8	6.7	0.0	40.1	0.0	0.0	0.7	12.4	0.0	0.1	0.8
EPS3063	42.3	1.8	7.2	0.0	30.1	0.0	0.0	0.1	16.5	0.0	0.1	0.3
EPS3065	47.9	1.6	9.9	0.0	32.6	0.0	0.0	0.2	7.0	0.0	0.0	0.3
EPS3066	33.0	1.5	6.9	0.0	50.2	0.0	0.0	0.1	7.4	0.0	0.0	0.4
EPS3071	34.2	0.9	10.5	0.0	50.1	0.0	0.0	0.0	3.4	0.0	0.4	0.3
EPS3073	38.6	1.6	8.6	0.0	38.6	0.0	0.0	0.1	10.9	0.0	0.1	0.5
EPS3075	49.2	1.8	12.1	0.0	31.7	0.0	0.0	0.0	4.3	0.0	0.0	0.3
EPS3076	45.4	1.9	12.8	0.0	34.3	0.0	0.0	0.1	4.4	0.0	0.0	0.1
EPS3077	46.8	1.8	10.4	0.0	35.0	0.0	0.0	0.1	4.6	0.0	0.0	0.4
Posidonia Shale												
RWEP6	16.8	0.0	0.5	8.4	13.1	0.0	1.9	41.2	1.4	1.7	0.0	3.7
RWEP8	15.6	0.0	0.5	5.5	7.3	0.0	1.6	52.2	0.9	1.1	0.0	3.7
RWEP10	14.3	0.0	1.0	5.7	12.4	0.0	1.0	43.9	1.9	1.0	0.0	4.8
RWEP14	13.1	0.0	0.9	4.7	13.1	0.0	0.7	43.9	1.9	0.7	0.0	3.7
Carboniferous Shale												
KB186-13	10.7	0.0	0.8	8.7	75.0	0.0	4.1	0.0	0.0	0.0	0.0	0.0
KB186-15	40.2	8.4	1.5	15.2	24.1	0.0	4.5	0.0	0.0	2.9	0.0	0.0
KB186-17	8.2	0.0	0.7	16.0	67.8	0.0	3.0	0.0	0.0	0.0	0.0	0.0
KB186-19	19.3	0.4	0.9	20.0	52.8	0.0	5.1	0.0	0.0	0.0	0.0	0.0
KB186-25	9.3	0.9	0.8	13.1	40.2	0.0	1.1	0.0	0.0	18.0	0.0	0.0
KB186-26	8.8	0.3	0.7	10.0	40.8	0.0	0.8	0.0	0.0	27.4	0.0	0.0
Bossier Shale												
SHSI 6-2	20.7	0.0	10.9	0.0	49.8	0.0	4.5	12.8	0.0	0.0	0.0	0.0
SHSI 1-6	18.8	0.0	9.9	0.0	54.3	0.0	4.9	10.9	0.0	0.0	0.0	0.0
SCN 3-6	10.9	0.0	5.7	0.0	25.2	0.0	2.3	53.9	0.0	0.0	0.0	0.0
SMY 4-2	7.1	0.0	3.8	0.0	9.1	0.0	0.8	78.1	0.0	0.0	0.0	0.0
BSA1	15.4	4.4	3.2	0.0	32.3	0.0	2.9	14.8	0.0	0.3	0.0	2.5
BSA2	13.5	1.6	4.2	0.0	45.2	0.0	4.9	2.2	0.0	0.5	0.0	5.2
BSA3	16.7	4.5	3.3	0.0	39.9	0.0	3.9	6.9	0.0	0.4	0.0	1.6
BSA4	14.6	5.8	3.8	0.0	33.7	0.0	3.3	10.2	0.0	0.4	0.0	1.1
Haynesville Shale												
SBI 8-2	27.9	0.0	10.0	1.3	31.4	0.0	1.3	25.3	0.0	0.0	0.0	0.0
SOM 4-4	27.9	0.0	10.1	1.0	24.6	0.0	1.0	30.4	0.0	0.0	0.0	0.0
SOM 9-2	27.8	0.0	10.0	1.6	39.4	0.0	1.6	16.5	0.0	0.0	0.0	0.0
HSA1	17.6	6.1	3.0	0.0	32.8	0.0	1.6	11.5	0.0	0.4	0.0	3.3
HSA2	11.4	3.5	2.2	0.0	18.3	0.0	1.5	35.5	0.0	0.0	0.0	1.7
HSA3	18.8	4.7	2.6	0.0	24.0	0.0	2.1	22.2	0.0	0.2	0.0	1.9

HSO1	23.9	0.0	8.6	1.9	46.0	0.0	1.9	9.6	1.0	0.0	0.0	1.9
HSJ2	24.1	0.0	8.7	1.9	46.3	0.0	1.9	9.7	1.0	0.0	0.0	1.9
Eagle Ford Shale												
EFS1	18.2	0.0	0.0	3.8	2.9	0.0	0.0	66.9	0.0	0.0	0.0	1.0
Jordan Oil Shale												
JS1	16.8	5.4	3.1	0.0	33.5	0.0	2.4	14.6	0.0	0.3	0.0	1.9
JS2	20.0	5.2	3.1	0.0	30.2	0.0	2.1	15.7	0.0	0.4	0.0	2.3
JS3	16.4	4.8	3.9	0.0	35.5	0.0	2.2	11.5	0.0	0.5	0.0	3.6
JS4	15.8	6.1	3.3	0.0	24.8	0.0	1.4	23.4	0.0	0.4	0.0	3.6
Newark Shale												
NS1	2.9	0.0	37.1	0.0	30.2	0.0	0.0	0.0	2.9	0.0	0.0	0.0

Table S 1. (continued)

Sample	**Anhydrite**	**Gypsum**	**Zirkon**	**Anatase**	**Apatite**	**Ankerite**	**Plagioclase**	**Buddingtonite**	**TOC**	**VRr**	**ρ**	**SLD**
	wt.%	wt.%	wt.%	wt.%	wt.%	wt.%	wt.%	wt.%	wt.%	%	g/cm^3	10E10 cm^{-2}
Opalinus Clay												
CCP01	0.9	0.7	0.0	0.0	0.0	0.0	0.0	0.0	1.2	0.45	2.71	3.767
CCP04	0.6	0.7	0.0	0.0	0.0	0.0	0.0	0.0	1.0	0.45	2.73	3.731
CCP05	0.6	0.6	0.0	0.0	0.0	0.0	0.0	0.0	1.0	0.45	2.72	3.736
CCP06	1.0	0.4	0.0	0.0	0.0	0.0	0.0	0.0	1.3	0.45	2.72	3.750
CCP07	1.0	0.8	0.0	0.0	0.0	0.0	0.0	0.0	1.5	0.45	2.72	3.724
CCP09	1.1	1.0	0.0	0.0	0.0	0.0	0.0	0.0	1.4	0.45	2.74	3.736
CCP10	1.0	0.7	0.0	0.0	0.0	0.0	0.0	0.0	1.2	0.45	2.73	3.764
CCP12	0.9	0.6	0.0	0.0	0.0	0.0	0.0	0.0	1.4	0.45	2.74	3.733
CCP14	1.0	0.4	0.0	0.0	0.0	0.0	0.0	0.0	1.1	0.45	2.74	3.708
Boom Clay												
BC-K4	0.0	0.5	0.0	0.7	0.0	0.0	0.0	0.0	0.3	0.3	2.71	3.764
BC-K10	0.0	0.0	0.0	0.6	0.0	0.0	0.0	0.0	0.2	0.3	2.66	3.782
BC-K11	0.0	0.0	0.0	0.7	0.0	0.0	0.0	0.0	0.2	0.3	2.65	3.762
BC-K2	0.0	0.6	0.0	0.7	0.0	0.0	0.0	0.0	0.2	0.3	2.69	3.755
BC-K9	0.0	0.3	0.0	0.7	0.0	0.0	0.0	0.0	0.2	0.3	2.66	3.669
Vale Shale												
VS1	0.0	0.0	0.0	0.0	0.0	0.0	0.0	0.0	1.0	0	2.63	3.885
VS2	0.0	0.0	0.0	0.0	0.0	0.0	0.0	0.0	1.0	0	2.60	3.704
VS3	0.0	0.0	0.0	0.0	0.0	0.0	0.0	0.0	1.0	0	2.62	3.717
Carmel Claystone												
NPS069	0.0	0.0	0.0	0.9	0.0	0.0	0.0	0.0	0.0	0	2.88	3.889

NPS073	0.0	0.0	0.0	0.9	0.0	0.0	0.0	0.0	0.0	0	2.76	3.869
NPS077	0.0	1.1	0.0	0.8	0.0	0.0	0.0	0.0	0.0	0	2.83	3.952
NPS080	0.0	0.3	0.0	0.8	0.0	0.0	0.0	0.0	0.0	0	2.85	3.969
NPS083	0.0	0.5	0.0	0.8	0.0	0.0	0.0	0.0	0.0	0	2.83	3.943
NPS086	0.0	0.2	0.0	0.7	0.0	0.0	0.0	0.0	0.0	0	2.87	4.039
NPS089	0.0	0.1	0.0	0.7	0.0	0.0	0.0	0.0	0.0	0	2.89	4.062
NPS095	0.0	0.1	0.0	0.7	0.0	0.0	0.0	0.0	0.0	0	2.88	4.043
Big Hole Carmel												
BH2CC16b	0.0	0.0	0.2	0.3	0.0	0.0	0.0	0.0	0.0	0	2.74	4.372
Entrada Siltstone												
EPS1004	0.0	0.0	0.4	0.2	0.3	0.0	0.0	0.0	0.0	0	2.72	4.146
EPS3049	0.0	0.0	0.5	0.2	0.3	0.0	0.0	0.0	0.0	0	2.73	4.115
EPS3057	0.0	0.0	0.4	0.0	0.3	0.0	0.0	0.0	0.0	0	2.77	4.180
EPS3058	0.0	0.0	0.4	0.2	0.3	0.0	0.0	0.0	0.0	0	2.72	4.146
EPS3059	0.0	0.0	0.4	0.0	0.3	0.0	0.0	0.0	0.0	0	2.73	4.147
EPS3061	0.0	0.0	0.4	0.4	0.3	0.0	0.0	0.0	0.0	0	2.75	4.164
EPS3062	0.0	0.0	0.6	0.0	0.3	0.0	0.0	0.0	0.0	0	2.76	4.161
EPS3063	0.0	0.0	0.5	0.4	0.6	0.0	0.0	0.0	0.0	0	2.74	4.231
EPS3065	0.0	0.0	0.7	0.0	0.2	0.0	0.0	0.0	0.0	0	2.73	4.111
EPS3066	0.0	0.0	0.5	0.0	0.2	0.0	0.0	0.0	0.0	0	2.74	4.049
EPS3071	0.0	0.0	0.1	0.2	0.2	0.0	0.0	0.0	0.0	0	2.73	3.988
EPS3073	0.0	0.0	0.7	0.0	0.4	0.0	0.0	0.0	0.0	0	2.74	4.134
EPS3075	0.0	0.0	0.4	0.1	0.3	0.0	0.0	0.0	0.0	0	2.71	4.054
EPS3076	0.0	0.0	0.6	0.3	0.2	0.0	0.0	0.0	0.0	0	2.71	4.036
EPS3077	0.0	0.0	0.7	0.3	0.3	0.0	0.0	0.0	0.0	0	2.73	4.062
Posidonia Shale												
RWEP6	0.0	2.3	0.0	0.3	0.0	0.5	1.4	0.0	6.1	0.6	2.71	4.056
RWEP8	0.0	1.4	0.0	0.1	0.0	0.2	1.3	0.0	8.1	0.6	2.67	4.114
RWEP10	0.0	1.0	0.0	1.2	0.0	3.8	3.3	0.0	4.4	0.9	2.78	4.187
RWEP14	0.0	2.4	0.0	2.6	0.0	0.7	4.6	0.0	5.9	1.5	2.71	4.025
Carboniferous Shale												
KB186-13	0.0	0.0	0.0	0.0	0.0	0.0	0.0	0.0	0.7	1.1	2.74	3.761
KB186-15	0.0	0.0	0.0	0.0	0.0	0.0	0.0	0.0	3.2	1.1	2.69	3.893
KB186-17	0.0	0.0	0.0	0.0	0.0	0.0	0.0	0.0	4.3	1.1	2.68	3.624
KB186-19	0.0	0.0	0.0	0.0	0.0	0.0	0.0	0.0	1.5	1.1	2.71	3.714
KB186-25	0.0	0.0	0.0	0.0	0.0	0.0	0.0	0.0	16.7	1.1	2.71	3.925
KB186-26	0.0	0.0	0.0	0.0	0.0	0.0	0.0	0.0	11.2	1.1	2.90	4.356
Bossier Shale												
SHSI 6-2	0.0	0.0	0.0	0.0	0.0	0.0	0.0	0.0	1.3	1.81	2.71	3.940

SHSI 1-6	0.0	0.0	0.0	0.0	0.0	0.0	0.0	0.0	1.3	1.79	2.72	3.916
SCN 3-6	0.0	0.0	0.0	0.0	0.0	0.0	0.0	0.0	2.0	2.26	2.69	4.263
SMY 4-2	0.0	0.0	0.0	0.0	0.0	0.0	0.0	0.0	1.1	2.15	2.69	4.491
BSA1	0.0	0.2	0.0	0.6	0.0	1.4	0.0	0.0	2.2	1.43	3.02	4.348
BSA2	0.0	0.3	0.0	0.9	0.0	0.5	0.0	0.0	1.9	1.43	3.10	4.197
BSA3	0.0	0.2	0.0	0.8	0.0	0.9	0.0	0.0	2.1	1.43	3.00	4.264
BSA4	0.9	0.1	0.0	0.4	0.0	2.7	0.0	0.0	2.3	1.43	3.01	4.351
Haynesville Shale												
SBI 8-2	0.0	0.0	0.0	0.0	0.0	0.0	0.0	0.0	2.8	2.42	2.66	4.040
SOM 4-4	0.0	0.0	0.0	0.0	0.0	0.0	0.0	0.0	5.0	2.53	2.62	4.038
SOM 9-2	0.0	0.0	0.0	0.0	0.0	0.0	0.0	0.0	3.0	2.58	2.66	3.953
HSA1	0.0	0.6	0.0	0.8	0.0	0.5	0.0	0.0	2.2	2.06	3.03	4.309
HSA2	0.0	0.2	0.0	0.3	0.0	2.0	0.0	0.0	2.4	2.06	3.00	4.543
HSA3	0.0	0.1	0.0	0.5	0.0	1.5	0.0	0.0	1.6	2.06	3.01	4.447
HSO1	0.0	1.0	0.0	0.0	0.0	0.0	0.0	0.0	4.3	2.06	2.69	3.848
HSJ2	0.0	1.0	0.0	0.0	0.0	0.0	0.0	0.0	3.5	2.06	2.71	3.867
Eagle Ford Shale												
EFS1	0.0	2.9	0.0	0.0	0.0	0.0	0.0	0.0	4.4	1.3	2.65	4.296
Jordan Oil Shale												
JS1	0.0	0.0	0.0	0.6	0.0	1.7	0.0	0.0	0.0	0.6	3.04	4.409
JS2	0.0	0.1	0.0	0.6	0.0	0.7	0.0	0.0	0.0	0.6	3.04	4.418
JS3	0.0	0.3	0.0	0.7	0.0	1.4	0.0	0.0	0.0	0.6	3.07	4.365
JS4	0.0	0.2	0.0	0.5	0.0	0.3	0.0	0.0	0.0	0.6	3.07	4.477
Newark Shale												
NS1	0.0	0.0	0.0	0.0	0.0	19.5	4.9	0.0	2.5	2.5	2.70	4.046

S2.3. Small Angle Neutron Scattering

Figure S 1 illustrates a typical SANS experiment. A flux of monochromatic neutrons- that travels in the straight trajectory of their wave vector k_0- is elastically scattered inside a sample of uniform thickness *h* and irradiated volume *V*. The magnitude of k_0 is $2\pi.\lambda^{-1}$, where λ is the neutron wavelength. The intensity *dI* scattered in direction *k* is measured; thereby the convention $k - k_0 = Q$, the scattering vector. The scattering vector is expressed by $Q = 4\pi sin\theta/\lambda$ (Radlinski 2006).

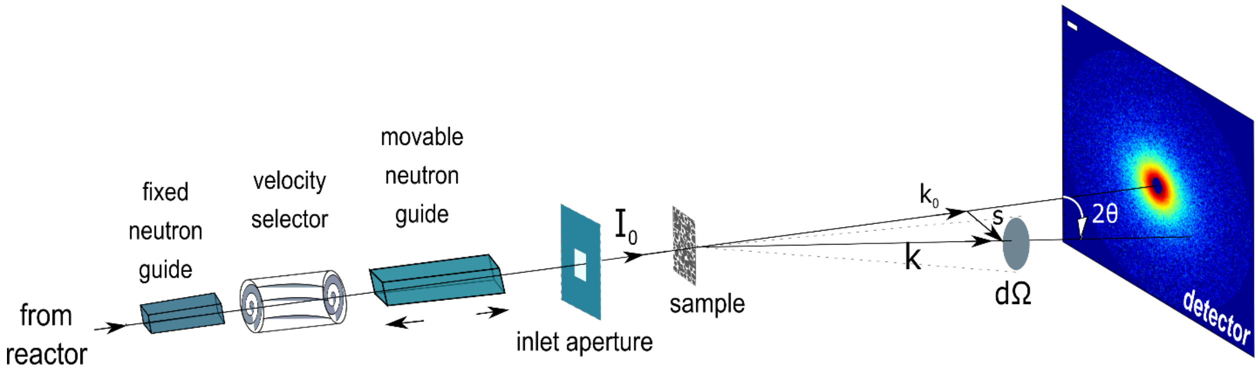

Figure S 1. Schematics of the SANS technique.

The incident flux of the scattering objects is denoted by Φ_0, i.e., $\Phi_0 = I_0/A$, where I_0 is the incident intensity (neutrons per second) and *A* is the beam cross sectional area at the sample position (Radlinski 2006). The scattered intensity monitored in the solid angle element *d*Ω targeted by the scattering vector *Q* can be expressed as:

$$dI \propto \Phi_0 \frac{d\Sigma}{d\Omega} d\Omega \quad \text{(S1)}$$

where $d\sigma$ is the elemental scattering cross section. The quantity $d\Sigma/d\Omega$ is called the differential cross section of scattering (Radlinski 2006). The aim of SANS experiments is to determine volume-averaged information on the spatial distribution of neutron scattering length density (SLD) in the sample from the measured $d\Sigma/d\Omega$ as a function of scattering vector *Q*; $\frac{d\Sigma}{d\Omega}(Q)$ or *I(Q)* (Melnichenko 2015). SLD is the key feature of this technique as well as for quantitative interpretation of SANS results and the SLD of a mixture is calculated as (Radlinski 2006):

$$\rho^* = \frac{N_A\, d}{M} \sum_j p_j \left(\sum_i s_i b_i\right)_j \quad \text{(S2)}$$

where N_A is Avogadro's number, *d* is the mass density, *M* is the atomic mass of the mixture, p_j is the proportion by molecular number of the component *j* in the mixture, and s_i and b_i are the proportions by number and coherent scattering amplitude of the nucleus *i* in the component *j*, respectively. The effective SLD of samples are provided in Table S 1and a mean value of each mudrock is listed in Table S 2.

Table S 2. Structural formula, mineral density (ρ), and scattering length density (SLD) for each individual mineral phase.

Mineral	Structural formula	ρ	SLD
		g/cc	10E10 cm^{-2}
Quartz	SiO2	2.65	4.186
Albite	NaAlSi3O8	2.62	3.969
K-Feldspar	KAlSi3O8	2.56	3.656

Kaolinite	Al2Si2O5(OH)4	2.63	3.22
Illite/Mus/I-S	K0.75Mg0.15Fe0.1Al1.75Al0.5Si3.5O10(OH)2	2.76	3.777
Montmorillonite	Na0.3Ca0.3Al2Mg2Si4O10(OH)2	2.35	3.272
Chlorite	Fe3.5Mg1.5Al(Si3Al)O10(OH)8	3.17	3.87
Calcite	CaCO3	2.71	4.69
Dolomite	CaMg(CO3)2	2.88	5.474
Siderite	FeCO3	3.96	6.898
Hematite	Fe2O3	5.225	7.156
Pyrite	FeS2	5.01	3.808
Anhydrite	CaSO4	2.98	4.056
Gypsum	CaSO4.2(H2O)	2.31	2.215
Zirkon	ZrSiO4	4.65	5.275
Anatase	TiO2	3.9	2.423
Apatite	Ca5(PO4)3F	3.19	4.35
Ankerite	CaFe0.6Mg0.3Mn0.1(CO3)2	3.05	5.316
Plagioclase	Na0.5Ca0.5Si3AlO8	2.68	3.964
TOC		1.3	1.5

*SLDs are taken from the NIST website (NIST 2015).

The scattering intensity $I(Q)$ has dimensions of reciprocal length [cm^{-1}] and can be obtained by the approximation of pore space as an arbitrary distribution of spheres of radius *r* (Radlinski et al. 2002). According to polydisperse spherical (PDSP) model, *I(Q)* is given by:

$$I(Q) = (\rho^*_{matrix} - \rho^*_{pore})^2 \frac{\varphi}{\bar{V}} \int_{R_{min}}^{R_{max}} V^2 f(r)\, P(Q)\, dr \qquad \text{(S3)}$$

In equation (S3), R_{max} and R_{min} are the maximum and minimum pore radii, respectively, $V \equiv V(r) = \frac{4}{3}\pi r^3$ is the volume of a sphere of radius *r* (pore volume), $\bar{V} = \int_{R_{min}}^{R_{max}} V(r)\, f(r)\, dr$ is the average pore volume, *f(r)* is the probability density of the pore size distribution, and *P(Q)* is the form factor for a sphere of radius r. Assume the pore space is fractal, the pore size distribution follows $f(r) \sim r^{-(1+D_f)}$. $f(r)$ is expressed as $f(r) = \frac{D_f}{R_{min}{}^{-D_f} - R_{max}{}^{-D_f}} R^{-(1+D_f)}$, which is valid for $R_{max} > R_{min} > 0$ and $D_f \in (-1, \infty)$ where $D_f = 6 + slope$. We developed the MATSAS software (Rezaeyan et al. 2021), which uses PDSP model for analysis of SANS data obtained from mudrocks. MATSAS provides a full suite of pore structure characterisation including specific surface area, porosity, pore volume, and pore size distribution by pore volume and pore area. The fractal concept is also used to obtain fractal dimension for a given range of scattering vectors (Radlinski 2006) e.g., the pore and surface fractal dimensions are obtained from 0.0003 – 0.003 Å^{-1} and 0.03 – 0.003 Å^{-1}, respectively (Rezaeyan et al. 2021). Figure S 2 illustrates the scattering data and fitted PDSPs for all mudrock samples.

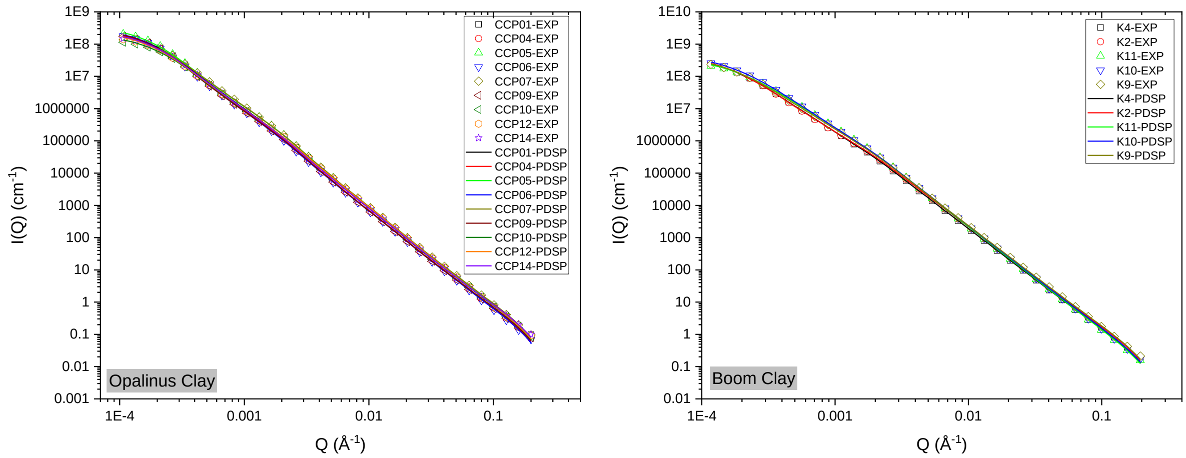

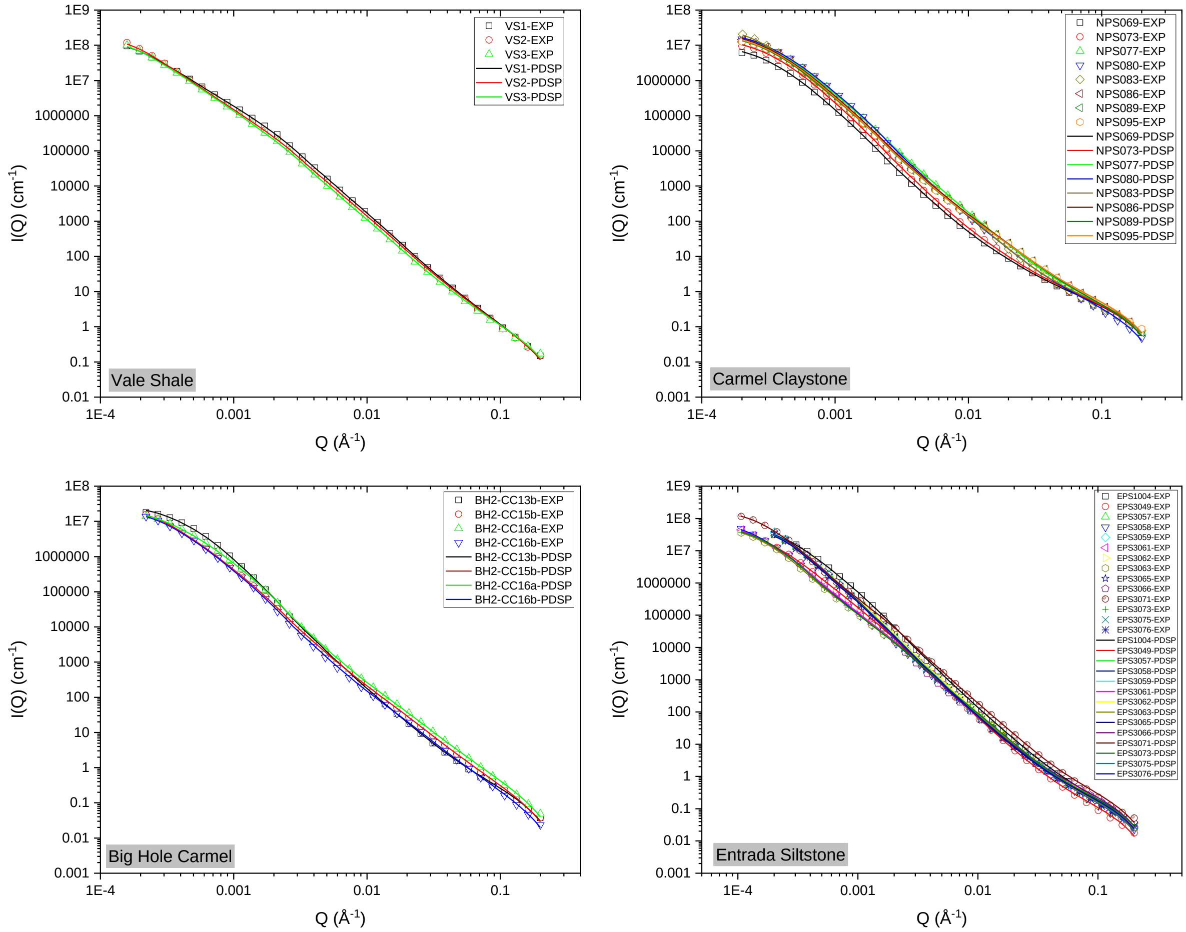

Figure S 2. Scattering profiles of mudrocks: the manipulated and PDSP model predicted using MATSAS.

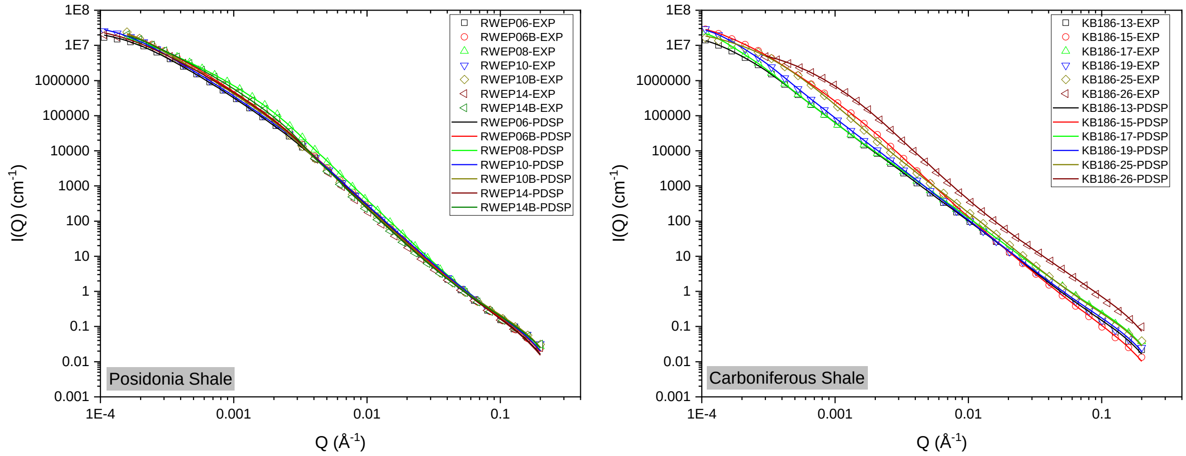

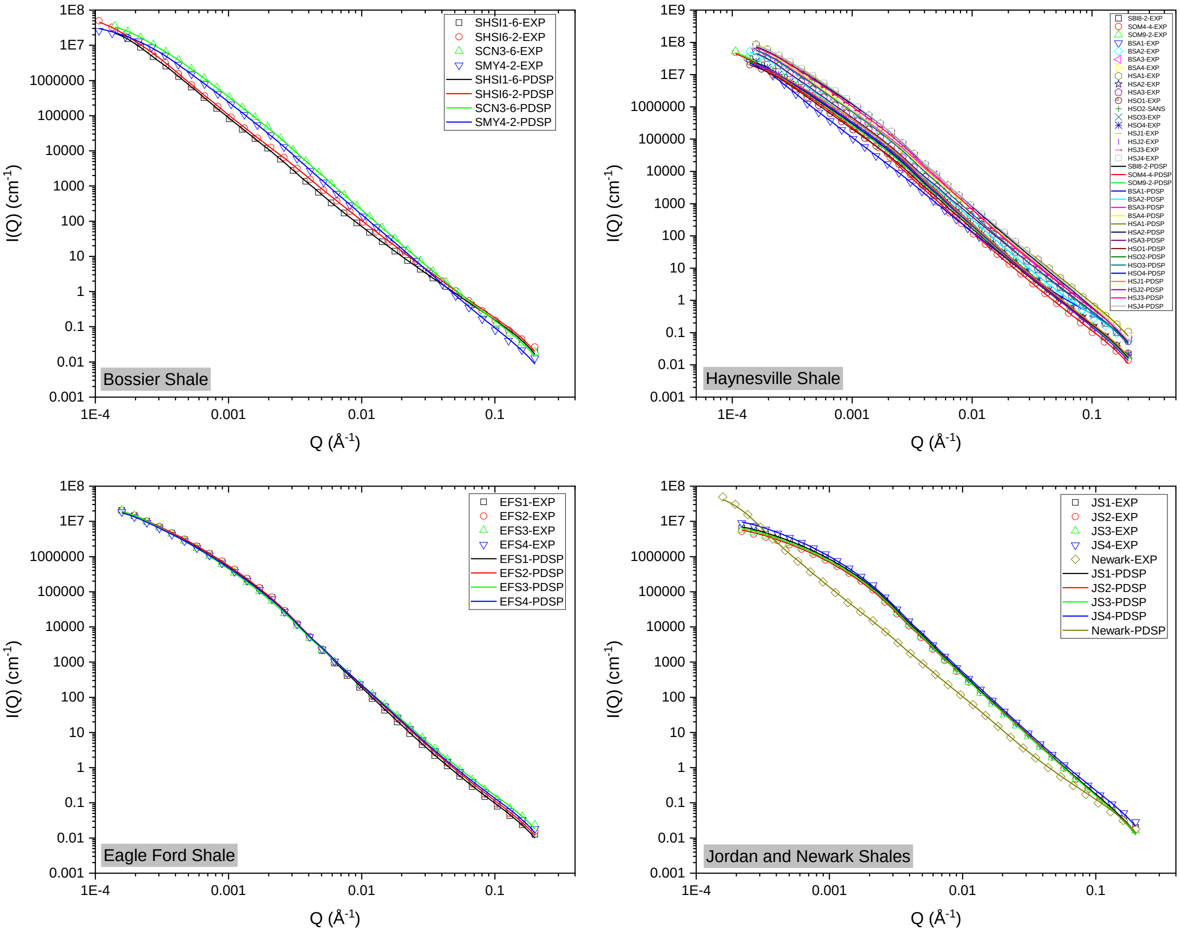

Figure S 2. (continued).

S3. Detailed Results

S3.1. Pore Size Dependent Transport Phenomena Data

Table S 3. Present-day burial depth (D_{pd}), temperature (T), intrinsic pore fluid pressure ($\bar{P}_p$) at current depth, fluid, fluid phase, molecular weight (MW), viscosity (μ_g), the exponent for the VSS model (ζ), viscosity index (η), the intermolecular collision coefficient for the VSS model (κ), MFP (δ), average pore size ($\bar{\chi}$), average Knudsen number ($\overline{Kn}$), and pore size boundaries of the dominant fluid flow regime for each individual sample.

Sample	**D_{pd}**	**T**	**$\bar{P}_p$**	**Fluid**	**MW**	**μ_g**	**Fluid Phase**	**ζ**	**η**	**κ**	**δ**	**Pore Size Boundaries (χ)**				**$\bar{\chi}$**	**$\overline{Kn}$**
	m	K	MPa		Kg/mol	Pa.s		-	-	-	nm	nm	nm	nm	nm	nm	
											Kn	0.001	0.1	10	100		
											Flow Regime	Continuum Flow	Slip Flow	Transition Flow	Free Molecular Flow		
Opalinus Clay																	
CCP01	250	290.5	2.5	H2	0.00202	8.817E-06	Supercritical	1.35	0.67	0.80	3.09	3094.9	30.9	0.31	0.031	10.5	0.29
CCP04	250	290.5	2.5	H2	0.00202	8.817E-06	Supercritical	1.35	0.67	0.80	3.09	3094.9	30.9	0.31	0.031	11.1	0.28
CCP05	250	290.5	2.5	H2	0.00202	8.817E-06	Supercritical	1.35	0.67	0.80	3.09	3094.9	30.9	0.31	0.031	11.4	0.27
CCP06	250	290.5	2.5	H2	0.00202	8.817E-06	Supercritical	1.35	0.67	0.80	3.09	3094.9	30.9	0.31	0.031	11.5	0.27
CCP07	250	290.5	2.5	H2	0.00202	8.817E-06	Supercritical	1.35	0.67	0.80	3.09	3094.9	30.9	0.31	0.031	10.8	0.29
CCP09	250	290.5	2.5	H2	0.00202	8.817E-06	Supercritical	1.35	0.67	0.80	3.09	3094.9	30.9	0.31	0.031	10.6	0.29
CCP10	250	290.5	2.5	H2	0.00202	8.817E-06	Supercritical	1.35	0.67	0.80	3.09	3094.9	30.9	0.31	0.031	10.5	0.29
CCP12	250	290.5	2.5	H2	0.00202	8.817E-06	Supercritical	1.35	0.67	0.80	3.09	3094.9	30.9	0.31	0.031	10.7	0.29
CCP14	250	290.5	2.5	H2	0.00202	8.817E-06	Supercritical	1.35	0.67	0.80	3.09	3094.9	30.9	0.31	0.031	9.8	0.32
Boom Clay																	
BC-K4	276	291.3	2.76	H2	0.00202	8.797E-06	Supercritical	1.35	0.67	0.80	2.80	2800.8	28.0	0.28	0.028	12.0	0.23
BC-K10	197	288.9	1.97	H2	0.00202	8.772E-06	Supercritical	1.35	0.67	0.80	3.90	3896.9	39.0	0.39	0.039	11.4	0.34
BC-K11	198	288.9	1.98	H2	0.00202	8.773E-06	Supercritical	1.35	0.67	0.80	3.88	3877.5	38.8	0.39	0.039	14.7	0.26
BC-K2	233	290.0	2.33	H2	0.00202	8.802E-06	Supercritical	1.35	0.67	0.80	3.31	3312.1	33.1	0.33	0.033	13.9	0.24
BC-K9	261	290.8	2.61	H2	0.00202	8.809E-06	Supercritical	1.35	0.67	0.80	2.96	2963.6	29.6	0.30	0.030	11.8	0.25
Våle Shale																	
VS1	2500	319.0	12	CO2	0.04401	5.393E-05	Supercritical	1.61	0.93	0.62	0.69	686.6	6.9	0.07	0.007	11.9	0.24

VS2	2500	319.0	12	CO2	0.04401	5.393E-05	Supercritical	1.61	0.93	0.62	0.69	686.6	6.9	0.07	0.007	10.6	0.27
VS3	2500	319.0	12	CO2	0.04401	5.393E-05	Supercritical	1.61	0.93	0.62	0.69	686.6	6.9	0.07	0.007	8.9	0.32
Carmel Claystone																	
NPS069	200	289.0	2	CO2	0.04401	1.477E-05	Vapour	1.61	0.93	0.62	1.07	1074.3	10.7	0.11	0.011	3.5	0.31
NPS073	200	289.0	2	CO2	0.04401	1.477E-05	Vapour	1.61	0.93	0.62	1.07	1074.3	10.7	0.11	0.011	4.1	0.26
NPS077	200	289.0	2	CO2	0.04401	1.477E-05	Vapour	1.61	0.93	0.62	1.07	1074.3	10.7	0.11	0.011	5.8	0.19
NPS080	200	289.0	2	CO2	0.04401	1.477E-05	Vapour	1.61	0.93	0.62	1.07	1074.3	10.7	0.11	0.011	7.0	0.15
NPS083	200	289.0	2	CO2	0.04401	1.477E-05	Vapour	1.61	0.93	0.62	1.07	1074.3	10.7	0.11	0.011	5.4	0.20
NPS086	200	289.0	2	CO2	0.04401	1.477E-05	Vapour	1.61	0.93	0.62	1.07	1074.3	10.7	0.11	0.011	4.9	0.22
NPS089	200	289.0	2	CO2	0.04401	1.477E-05	Vapour	1.61	0.93	0.62	1.07	1074.3	10.7	0.11	0.011	5.1	0.21
NPS095	200	289.0	2	CO2	0.04401	1.477E-05	Vapour	1.61	0.93	0.62	1.07	1074.3	10.7	0.11	0.011	4.7	0.23
Big Hole Carmel																	
BH2CC16b	200	289.0	2	CO2	0.04401	1.477E-05	Vapour	1.61	0.93	0.62	1.07	1074.3	10.7	0.11	0.011	10.4	0.10
Entrada Siltstone																	
EPS1004	220	289.6	2.2	CO2	0.04401	1.46E-05	Vapour	1.61	0.93	0.62	0.97	965.8	9.7	0.10	0.010	12.0	0.12
EPS3049	222	289.7	2.22	CO2	0.04401	1.46E-05	Vapour	1.61	0.93	0.62	0.96	957.2	9.6	0.10	0.010	8.8	0.16
EPS3057	222	289.7	2.22	CO2	0.04401	1.46E-05	Vapour	1.61	0.93	0.62	0.96	957.2	9.6	0.10	0.010	8.9	0.16
EPS3058	222	289.7	2.22	CO2	0.04401	1.46E-05	Vapour	1.61	0.93	0.62	0.96	957.2	9.6	0.10	0.010	6.4	0.22
EPS3059	222	289.7	2.22	CO2	0.04401	1.46E-05	Vapour	1.61	0.93	0.62	0.96	957.2	9.6	0.10	0.010	7.8	0.18
EPS3061	222	289.7	2.22	CO2	0.04401	1.46E-05	Vapour	1.61	0.93	0.62	0.96	957.2	9.6	0.10	0.010	5.7	0.25
EPS3062	222	289.7	2.22	CO2	0.04401	1.46E-05	Vapour	1.61	0.93	0.62	0.96	957.2	9.6	0.10	0.010	8.1	0.17
EPS3063	222	289.7	2.22	CO2	0.04401	1.46E-05	Vapour	1.61	0.93	0.62	0.96	957.2	9.6	0.10	0.010	6.1	0.23
EPS3065	222	289.7	2.22	CO2	0.04401	1.46E-05	Vapour	1.61	0.93	0.62	0.96	957.2	9.6	0.10	0.010	7.6	0.19
EPS3066	222	289.7	2.22	CO2	0.04401	1.46E-05	Vapour	1.61	0.93	0.62	0.96	957.2	9.6	0.10	0.010	7.1	0.20
EPS3071	222	289.7	2.22	CO2	0.04401	1.46E-05	Vapour	1.61	0.93	0.62	0.96	957.2	9.6	0.10	0.010	8.2	0.17
EPS3073	222	289.7	2.22	CO2	0.04401	1.46E-05	Vapour	1.61	0.93	0.62	0.96	957.2	9.6	0.10	0.010	5.3	0.27
EPS3075	222	289.7	2.22	CO2	0.04401	1.46E-05	Vapour	1.61	0.93	0.62	0.96	957.2	9.6	0.10	0.010	8.9	0.16

EPS3076	222	289.7	2.22	CO2	0.04401	1.46E-05	Vapour	1.61	0.93	0.62	0.96	957.2	9.6	0.10	0.010	8.1	0.17
Posidonia Shale																	
RWEP6	2500	358.0	25	CH4	0.01604	1.988E-05	Supercritical	1.60	0.84	0.68	0.23	233.4	2.3	0.02	0.002	12.9	0.02
RWEP10	2500	358.0	25	CH4	0.01604	1.988E-05	Supercritical	1.60	0.84	0.68	0.23	233.4	2.3	0.02	0.002	11.2	0.02
RWEP14	2500	358.0	25	CH4	0.01604	1.988E-05	Supercritical	1.60	0.84	0.68	0.23	233.4	2.3	0.02	0.002	11.2	0.02
Carboniferous Shale																	
KB186-13	1185	318.6	11.85	CH4	0.01604	1.988E-05	Supercritical	1.60	0.84	0.68	0.46	464.5	4.6	0.05	0.005	5.9	0.04
KB186-15	1187	318.6	11.87	CH4	0.01604	1.988E-05	Supercritical	1.60	0.84	0.68	0.46	463.8	4.6	0.05	0.005	14.0	0.02
KB186-17	1191	318.7	11.91	CH4	0.01604	1.988E-05	Supercritical	1.60	0.84	0.68	0.46	462.3	4.6	0.05	0.005	4.8	0.05
KB186-19	1192	318.8	11.92	CH4	0.01604	1.988E-05	Supercritical	1.60	0.84	0.68	0.46	462.0	4.6	0.05	0.005	6.1	0.04
KB186-25	1197	318.9	11.97	CH4	0.01604	1.988E-05	Supercritical	1.60	0.84	0.68	0.46	460.1	4.6	0.05	0.005	6.8	0.03
KB186-26	1197	318.9	11.97	CH4	0.01604	1.988E-05	Supercritical	1.60	0.84	0.68	0.46	460.1	4.6	0.05	0.005	6.8	0.03
Bossier Shale																	
SHSI 6-2	3661	392.8	36.61	CH4	0.01604	2.223E-05	Supercritical	1.60	0.84	0.68	0.19	186.7	1.9	0.02	0.002	6.2	0.03
SHSI 1-6	3673	393.2	36.73	CH4	0.01604	2.317E-05	Supercritical	1.60	0.84	0.68	0.19	194.0	1.9	0.02	0.002	6.7	0.03
SCN 3-6	3746	395.4	37.46	CH4	0.01604	2.335E-05	Supercritical	1.60	0.84	0.68	0.19	192.3	1.9	0.02	0.002	14.4	0.01
SMY 4-2	3762	395.9	37.62	CH4	0.01604	2.339E-05	Supercritical	1.60	0.84	0.68	0.19	191.9	1.9	0.02	0.002	16.5	0.01
BSA1	4000	403.0	40	CH4	0.01604	2.401E-05	Supercritical	1.60	0.84	0.68	0.19	186.9	1.9	0.02	0.002	4.2	0.01
BSA2	3500	388.0	35	CH4	0.01604	2.223E-05	Supercritical	1.60	0.84	0.68	0.19	194.1	1.9	0.02	0.002	8.4	0.01
BSA3	3000	373.0	30	CH4	0.01604	2.223E-05	Supercritical	1.60	0.84	0.68	0.22	222.0	2.2	0.02	0.002	10.9	0.01
BSA4	2950	371.5	29.5	CH4	0.01604	2.223E-05	Supercritical	1.60	0.84	0.68	0.23	225.3	2.3	0.02	0.002	8.7	0.01
Haynesville Shale																	
SBI 8-2	3766	396.0	37.66	CH4	0.01604	2.34E-05	Supercritical	1.60	0.84	0.68	0.19	191.8	1.9	0.02	0.002	14.7	0.01
SOM 4-4	4041	404.2	40.41	CH4	0.01604	2.401E-05	Supercritical	1.60	0.84	0.68	0.19	185.3	1.9	0.02	0.002	12.9	0.01
SOM 9-2	4054	404.6	40.54	CH4	0.01604	2.404E-05	Supercritical	1.60	0.84	0.68	0.19	185.0	1.9	0.02	0.002	12.3	0.02
HSA1	2900	370.0	29	CH4	0.01604	2.223E-05	Supercritical	1.60	0.84	0.68	0.23	228.7	2.3	0.02	0.002	11.0	0.02

HSA2	2500	358.0	25	CH4	0.01604	2.223E-05	Supercritical	1.60	0.84	0.68	0.26	261.0	2.6	0.03	0.003	14.1	0.02
HSA3	4200	409.0	42	CH4	0.01604	2.401E-05	Supercritical	1.60	0.84	0.68	0.18	179.3	1.8	0.02	0.002	8.9	0.02
HSO1	4450	416.5	44.5	CH4	0.01604	2.401E-05	Supercritical	1.60	0.84	0.68	0.17	170.8	1.7	0.02	0.002	9.6	0.02
HSJ2	4300	412.0	43	CH4	0.01604	2.401E-05	Supercritical	1.60	0.84	0.68	0.18	175.8	1.8	0.02	0.002	14.7	0.02
Eagle Ford Shale																	
EFS1	3700	394.0	37	CH4	0.01604	2.392E-05	Supercritical	1.60	0.84	0.68	0.20	199.05	1.9905	0.02	0.002	23.5	0.01
Jordan Oil Shale																	
JS1	1750	335.5	17.5	CH4	0.01604	1.988E-05	Supercritical	1.60	0.84	0.68	0.37	365.5	3.655	0.04	0.004	26.0	0.01
Newark Shale																	
NS1	3962	401.9	39.62	CH4	0.01604	2.383E-05	Supercritical	1.60	0.84	0.68	0.19	187.01	1.8701	0.02	0.002	9.8	0.01

ζ and η are obtained by Bird (1994).

S3.2. Pore Characteristics Data

Table S 4. Pore characteristics of the individual samples: fractal dimensions (D), slope of scattering profile (m), incoherent scattering background (SANS), specific surface area (SSA), pore volume (V_P), porosity (Φ), and average (mean) pore size ($\bar{\chi}$).

Sample	**D_p**	**D_s**	**D_f**	**m**	**I_{BG}**	**SSA**	**SSA**	**SSA**	**SSA**	**V_p**	**V_p**	**V_p**	**V_p**	**Φ**	**Φ**	**Φ**	**Φ**	**$\bar{\chi}$**
					SANS	cuml.	macro	meso	nano	cuml.	macro	meso	nano	cuml.	macro	meso	nano	
					cm^{-1}	m^2/g	m^2/g	m^2/g	m^2/g	cm^3/g	cm^3/g	cm^3/g	cm^3/g	%	%	%	%	nm
Opalinus Clay																		
CCP01	2.75	2.88	2.94	-3.06	1.15	33.5	1.4	32.1	27.8	0.088	0.054	0.034	0.019	23.9	14.7	9.1	5.0	10.54
CCP04	2.74	2.89	2.93	-3.07	0.95	27.9	1.2	26.6	22.9	0.078	0.049	0.029	0.016	21.1	13.2	7.9	4.2	11.13
CCP05	2.68	2.87	2.92	-3.08	1.19	34.9	1.6	33.3	28.6	0.100	0.063	0.036	0.020	27.1	17.2	9.9	5.3	11.44
CCP06	2.79	2.89	2.93	-3.07	0.95	25.7	1.1	24.5	20.9	0.073	0.046	0.027	0.014	19.9	12.6	7.4	3.9	11.45
CCP07	2.74	2.88	2.93	-3.07	1.29	37.3	1.6	35.7	30.7	0.101	0.062	0.039	0.021	27.4	16.9	10.5	5.7	10.81
CCP09	2.74	2.88	2.94	-3.06	0.93	28.8	1.2	27.6	24.0	0.076	0.047	0.029	0.016	20.8	12.9	7.9	4.4	10.55
CCP10	2.69	2.86	2.96	-3.04	1.06	31.7	1.4	30.3	26.1	0.083	0.051	0.033	0.018	22.7	13.8	8.9	4.8	10.54
CCP12	2.70	2.88	2.98	-3.02	1.11	33.2	1.5	31.7	27.1	0.089	0.054	0.035	0.018	24.2	14.6	9.6	5.0	10.68
CCP14	2.77	2.91	2.95	-3.05	0.56	36.3	1.4	34.9	30.4	0.089	0.053	0.036	0.020	24.2	14.5	9.8	5.4	9.79
Boom Clay																		
BC-K4	2.62	2.85	3.04	-2.96	0.01	36.2	2.1	34.1	28.0	0.109	0.067	0.042	0.020	29.4	18.1	11.3	5.4	12.05
BC-K10	2.51	2.86	3.08	-2.92	0.01	42.7	2.3	40.4	33.2	0.122	0.072	0.049	0.024	32.2	19.1	13.1	6.2	11.38

BC-K11	2.60	2.77	2.99	-3.01	0.01	35.2	2.6	32.5	26.0	0.129	0.086	0.043	0.019	34.1	22.7	11.3	5.0	14.69
BC-K2	2.65	2.80	2.99	-3.01	0.01	38.7	2.6	36.1	29.1	0.135	0.088	0.047	0.021	36.1	23.6	12.5	5.6	13.92
BC-K9	2.56	2.85	3.05	-2.95	0.01	47.9	2.7	45.2	37.2	0.141	0.086	0.055	0.026	37.4	22.7	14.7	7.0	11.77
Våle Shale																		
VS1	2.35	2.65	2.96	-3.04	1.12	49.5	3.2	46.3	40.0	0.147	0.097	0.050	0.026	38.5	25.4	13.1	6.7	11.88
VS2	2.49	2.72	2.96	-3.04	1.31	53.4	2.8	50.6	44.3	0.141	0.089	0.052	0.028	36.5	23.0	13.5	7.3	10.56
VS3	2.61	2.73	2.92	-3.08	1.16	55.3	2.2	53.1	48.1	0.123	0.075	0.048	0.029	32.0	19.5	12.4	7.5	8.86
Carmel Claystone																		
NPS069	3.40	3.23	2.73	-3.27	0.09	17.7	0.1	17.6	17.3	0.015	0.005	0.010	0.009	4.4	1.5	3.0	2.7	3.48
NPS073	3.47	3.15	2.64	-3.36	0.09	18.9	0.1	18.8	18.4	0.019	0.008	0.011	0.010	5.4	2.2	3.1	2.8	4.11
NPS077	3.17	2.90	2.74	-3.26	0.14	18.8	0.3	18.5	17.7	0.027	0.014	0.013	0.010	7.6	4.1	3.6	2.8	5.75
NPS080	3.19	2.88	2.62	-3.38	0.11	13.5	0.3	13.3	12.7	0.024	0.014	0.009	0.007	6.7	4.1	2.6	2.1	6.98
NPS083	2.85	2.82	2.85	-3.15	0.05	6.8	0.1	6.7	6.4	0.009	0.005	0.004	0.003	2.6	1.3	1.3	1.0	5.37
NPS086	3.29	3.15	2.78	-3.22	0.14	20.5	0.2	20.3	19.4	0.025	0.012	0.014	0.011	7.3	3.3	3.9	3.1	4.95
NPS089	3.29	3.20	2.80	-3.20	0.11	17.1	0.2	17.0	16.1	0.022	0.010	0.012	0.009	6.4	2.9	3.4	2.6	5.14
NPS095	3.34	3.19	2.79	-3.21	0.12	20.9	0.2	20.7	19.8	0.024	0.011	0.014	0.011	7.0	3.1	4.0	3.1	4.68
Big Hole Carmel																		
BH2CC16b	3.16	3.04	2.73	-3.27	0.02	6.5	0.2	6.3	5.6	0.017	0.011	0.006	0.004	4.6	3.0	1.6	1.0	10.36
Entrada Siltstone																		
EPS1004	3.34	2.71	2.55	-3.45	0.09	7.6	0.3	7.4	6.9	0.023	0.017	0.006	0.004	6.2	4.7	1.5	1.1	11.96
EPS3049	3.04	2.64	2.66	-3.34	0.04	4.6	0.1	4.4	4.2	0.010	0.007	0.003	0.002	2.7	1.9	0.8	0.6	8.82
EPS3057	3.52	2.88	2.59	-3.41	0.07	7.1	0.1	6.9	6.6	0.016	0.011	0.005	0.004	4.4	3.0	1.3	1.0	8.92
EPS3058	2.93	2.83	2.87	-3.13	0.02	6.3	0.1	6.1	5.8	0.010	0.006	0.004	0.003	2.7	1.5	1.2	0.9	6.39
EPS3059	3.47	2.83	2.52	-3.48	0.06	8.6	0.1	8.5	8.2	0.017	0.011	0.005	0.004	4.5	3.1	1.5	1.2	7.75
EPS3061	2.89	2.83	2.86	-3.14	0.04	7.5	0.1	7.3	7.0	0.011	0.006	0.005	0.004	2.9	1.6	1.4	1.0	5.70
EPS3062	3.32	2.83	2.58	-3.42	0.06	8.2	0.2	8.1	7.7	0.017	0.011	0.005	0.004	4.6	3.1	1.5	1.2	8.08
EPS3063	2.80	2.82	2.91	-3.09	0.05	6.2	0.1	6.1	5.8	0.009	0.005	0.004	0.003	2.6	1.4	1.2	0.9	6.07
EPS3065	3.41	2.82	2.52	-3.48	0.06	8.6	0.1	8.5	8.2	0.016	0.011	0.005	0.004	4.5	3.0	1.4	1.2	7.63
EPS3066	3.64	3.01	2.55	-3.45	0.09	9.4	0.1	9.3	8.9	0.017	0.011	0.006	0.005	4.6	2.9	1.7	1.4	7.15
EPS3071	2.88	2.77	2.79	-3.21	0.08	12.7	0.3	12.4	11.7	0.026	0.017	0.009	0.007	7.1	4.6	2.5	1.8	8.19
EPS3073	2.87	2.89	2.93	-3.07	0.06	8.4	0.1	8.3	7.9	0.011	0.005	0.006	0.004	3.0	1.5	1.5	1.2	5.27
EPS3075	3.29	2.78	2.57	-3.43	0.07	7.1	0.2	7.0	6.7	0.016	0.011	0.005	0.004	4.3	3.0	1.3	1.0	8.88
EPS3076	3.34	2.81	2.57	-3.43	0.08	7.7	0.1	7.6	7.3	0.016	0.011	0.005	0.004	4.3	2.9	1.4	1.1	8.08
Posidonia Shale																		
RWEP6	2.50	2.49	2.91	-3.09	0.15	6.9	0.5	6.3	5.6	0.022	0.016	0.006	0.003	6.0	4.3	1.7	0.9	12.93
RWEP10	2.50	2.52	2.92	-3.08	0.05	7.8	0.5	7.3	6.6	0.022	0.015	0.007	0.004	6.1	4.3	1.8	1.1	11.25
RWEP14	2.43	2.45	2.77	-3.23	0.13	8.6	0.5	8.1	7.5	0.024	0.018	0.006	0.004	6.5	4.8	1.7	1.2	11.24
Carboniferous Shale																		
KB186-13	2.88	3.18	3.19	-2.81	0.14	6.8	0.1	6.6	6.0	0.010	0.004	0.006	0.004	2.7	1.1	1.7	1.0	5.90

KB186-15	2.83	2.67	2.79	-3.21	0.10	4.3	0.3	4.0	3.5	0.015	0.011	0.004	0.002	4.1	2.9	1.1	0.6	14.05
KB186-17	2.82	3.27	3.27	-2.73	0.16	13.1	0.2	12.9	11.9	0.016	0.005	0.011	0.007	4.2	1.3	2.9	1.9	4.76
KB186-19	2.94	3.09	3.09	-2.91	0.13	8.2	0.2	8.1	7.3	0.013	0.006	0.007	0.004	3.4	1.5	1.9	1.2	6.14
KB186-25	3.23	3.04	2.97	-3.03	0.30	10.4	0.2	10.1	9.2	0.018	0.009	0.009	0.005	4.8	2.4	2.4	1.5	6.84
KB186-26	2.46	2.83	2.95	-3.05	0.07	21.6	0.6	21.0	19.4	0.037	0.019	0.018	0.012	10.7	5.6	5.1	3.6	6.84
Bossier Shale																		
SHSI 6-2	3.01	3.11	2.95	-3.05	0.09	6.4	0.1	6.3	5.8	0.010	0.005	0.005	0.004	2.7	1.3	1.4	1.0	6.23
SHSI 1-6	3.01	3.04	3.00	-3.00	0.04	7.5	0.1	7.3	6.7	0.012	0.006	0.006	0.004	3.4	1.7	1.7	1.1	6.68
SCN 3-6	2.91	2.72	2.81	-3.19	0.09	5.1	0.3	4.8	4.0	0.018	0.013	0.005	0.003	4.9	3.5	1.4	0.7	14.44
SMY 4-2	2.93	2.77	2.84	-3.16	0.02	2.8	0.2	2.6	2.1	0.012	0.008	0.003	0.001	3.1	2.3	0.9	0.4	16.51
BSA1	2.65	3.08	3.09	-2.91	0.04	12.6	0.1	12.5	11.9	0.013	0.005	0.009	0.007	4.0	1.4	2.6	2.0	4.22
BSA2	2.56	2.74	2.91	-3.09	0.05	12.2	0.4	11.8	10.8	0.026	0.016	0.010	0.006	7.9	4.8	3.1	2.0	8.40
BSA3	2.63	2.80	2.95	-3.05	0.31	16.8	0.9	15.9	13.7	0.046	0.028	0.017	0.009	13.6	8.5	5.1	2.7	10.86
BSA4	2.73	2.90	2.96	-3.04	0.18	21.5	0.7	20.8	18.4	0.047	0.027	0.020	0.012	14.0	8.0	6.0	3.5	8.66
Haynesville Shale																		
SBI 8-2	2.56	2.64	2.81	-3.19	0.08	6.3	0.5	5.8	5.0	0.023	0.017	0.006	0.003	6.2	4.5	1.7	0.9	14.75
SOM 4-4	2.80	2.77	2.83	-3.17	0.12	4.4	0.2	4.1	3.6	0.014	0.010	0.004	0.002	3.7	2.6	1.1	0.6	12.88
SOM 9-2	2.65	2.73	2.87	-3.13	0.12	6.2	0.4	5.9	5.1	0.019	0.013	0.006	0.003	5.1	3.4	1.6	0.9	12.28
HSA1	2.63	2.85	2.88	-3.12	0.93	23.8	1.1	22.6	19.5	0.066	0.042	0.024	0.013	19.8	12.7	7.2	4.0	11.05
HSA2	2.51	2.74	2.87	-3.13	0.71	15.0	1.0	13.9	11.7	0.053	0.037	0.016	0.008	15.8	10.9	4.9	2.5	14.12
HSA3	2.65	2.92	2.96	-3.04	0.39	12.4	0.4	11.9	10.5	0.028	0.016	0.012	0.007	8.3	4.7	3.6	2.1	8.94
HSO1	2.61	2.79	2.93	-3.07	0.06	6.8	0.3	6.5	5.8	0.016	0.010	0.006	0.004	4.4	2.7	1.7	1.0	9.64
HSJ2	2.60	2.67	2.82	-3.18	0.01	6.1	0.4	5.6	4.8	0.022	0.016	0.006	0.003	6.1	4.3	1.7	0.9	14.75
Eagle Ford Shale																		
EFS1	2.55	2.40	2.60	-3.40	0.06	3.4	0.4	3.0	2.7	0.020	0.017	0.003	0.002	5.4	4.5	0.8	0.4	23.45
Jordan Oil Shale																		
JS1	1.96	2.45	2.83	-3.17	0.23	4.6	0.8	3.8	3.0	0.030	0.025	0.005	0.002	9.1	7.5	1.6	0.6	25.99
JS2	1.96	2.55	2.88	-3.12	0.24	4.1	0.6	3.5	2.6	0.025	0.020	0.005	0.002	7.7	6.1	1.6	0.6	24.45
JS3	1.96	2.47	2.84	-3.16	0.20	4.2	0.7	3.5	2.7	0.027	0.022	0.005	0.002	8.3	6.8	1.5	0.6	25.78
JS4	2.08	2.46	2.79	-3.21	0.20	6.1	0.8	5.3	4.4	0.034	0.027	0.006	0.003	10.3	8.4	2.0	0.9	22.00
Newark Shale																		
NS1	3.01	2.83	2.87	-3.13	0.01	5.0	0.2	4.9	4.4	0.012	0.008	0.004	0.003	3.3	2.2	1.2	0.7	9.81

S3.3. Fractal Models Data

Table S 5. Darcy permeabilities calculated using the fractal model for each individual sample; minimum pore size (χ_{min}), mean pore size ($\bar{\chi}$), maximum pore size (χ_{max}), porosity (Φ), fractal dimension (D_f), tortuosity (τ), Straight length of capillary tube (L_0), fractal tortuosity dimension (D_τ), and Darcy permeability (K_D).

Sample	χ_{min}	$\bar{\chi}$	χ_{max}	Φ	D_f	τ	L_0	D_τ	K_D
	nm	nm	nm	-	-	-	nm	-	m^2
Opalinus Clay									
CCP01	2500	2510.5	5000	0.009	2.67	54.79	72862	1.81	5.11E-22
CCP04	2500	2511.1	5000	0.009	2.66	58.52	75144	1.80	4.10E-22
CCP05	2500	2511.4	5000	0.010	2.66	49.98	69301	1.82	7.67E-22
CCP06	2500	2511.5	5000	0.008	2.67	61.95	77425	1.80	3.23E-22
CCP07	2500	2510.8	5000	0.010	2.67	52.12	70943	1.82	6.32E-22
CCP09	2500	2510.6	5000	0.008	2.67	59.53	75939	1.80	3.74E-22
CCP10	2500	2510.5	5000	0.009	2.69	54.42	72975	1.81	4.89E-22
CCP12	2500	2510.7	5000	0.010	2.71	51.00	70926	1.82	5.93E-22
CCP14	2500	2509.8	5000	0.010	2.69	50.99	70476	1.82	6.47E-22
Boom Clay									
BC-K4	2500	2512.0	5000	0.012	2.77	43.06	65970	1.85	9.54E-22
BC-K10	2500	2511.4	5000	0.012	2.76	42.05	65015	1.85	1.08E-21
BC-K11	2500	2514.7	5000	0.012	2.77	42.46	65562	1.85	9.94E-22
BC-K2	2500	2513.9	5000	0.014	2.83	36.38	61385	1.88	1.53E-21
BC-K9	2500	2511.8	5000	0.014	2.77	37.40	61399	1.87	1.66E-21
Vale Shale									
VS1	2500	2511.9	5000	0.013	2.76	39.92	63246	1.86	1.35E-21
VS2	2500	2510.6	5000	0.012	2.76	42.06	65061	1.85	1.07E-21
VS3	2500	2508.9	5000	0.011	2.72	44.44	66226	1.84	9.97E-22
Carmel Claystone									
NPS069	2500	2503.5	5000	0.002	1.72	279.66	143367	1.61	9.44E-24
NPS073	2500	2504.1	5000	0.002	1.64	266.07	138685	1.61	1.32E-23
NPS077	2500	2505.8	5000	0.003	1.73	196.43	120234	1.64	3.52E-23
NPS080	2500	2507.0	5000	0.002	1.62	212.89	123728	1.63	3.21E-23

NPS083	2500	2505.4	5000	0.001	1.83	337.87	159484	1.60	3.75E-24
NPS086	2500	2504.9	5000	0.002	1.77	209.28	124584	1.63	2.59E-23
NPS089	2500	2505.1	5000	0.002	1.79	214.52	126418	1.63	2.27E-23
NPS095	2500	2504.7	5000	0.002	1.78	214.53	126305	1.63	2.30E-23
Big Hole Carmel									
BH2CC16b	2500	2510.4	5000	0.002	1.64	292.72	145452	1.60	9.22E-24
Entrada Siltstone									
EPS1004	2500	2512.0	5000	0.002	1.39	295.84	143051	1.59	1.34E-23
EPS3049	2500	2508.8	5000	0.001	1.49	351.07	157236	1.58	5.94E-24
EPS3057	2500	2508.9	5000	0.002	1.43	304.57	145623	1.59	1.13E-23
EPS3058	2500	2506.4	5000	0.001	1.68	370.18	164307	1.59	3.52E-24
EPS3059	2500	2507.8	5000	0.001	1.37	336.10	152238	1.58	8.58E-24
EPS3061	2500	2505.7	5000	0.002	1.68	324.99	153910	1.60	5.78E-24
EPS3062	2500	2508.1	5000	0.002	1.43	313.02	147586	1.59	1.03E-23
EPS3063	2500	2506.1	5000	0.001	1.72	389.00	169208	1.58	2.69E-24
EPS3065	2500	2507.6	5000	0.001	1.37	341.90	153499	1.58	8.09E-24
EPS3066	2500	2507.1	5000	0.002	1.40	331.57	151552	1.59	8.64E-24
EPS3071	2500	2508.2	5000	0.002	1.61	211.84	123342	1.63	3.31E-23
EPS3073	2500	2505.3	5000	0.001	1.74	360.58	163172	1.59	3.48E-24
EPS3075	2500	2508.9	5000	0.002	1.41	309.06	146490	1.59	1.10E-23
EPS3076	2500	2508.1	5000	0.002	1.42	312.83	147414	1.59	1.05E-23
Posidonia Shale									
RWEP6	250	262.9	5000	0.011	2.91	46.06	70923	2.32	1.71E-23
RWEP10	250	261.2	5000	0.011	2.92	45.35	70631	2.32	1.72E-23
RWEP14	250	261.2	5000	0.012	2.77	42.49	65499	2.32	3.88E-23
Carboniferous Shale									
KB186-13	250	255.9	5000	0.005	2.75	95.42	98248	2.23	2.18E-24

KB186-15	250	264.0	5000	0.007	2.79	74.56	87711	2.26	4.52E-24
KB186-17	250	254.8	5000	0.007	2.74	72.52	85317	2.26	6.13E-24
KB186-19	250	256.1	5000	0.007	2.78	75.89	88175	2.26	4.51E-24
KB186-25	250	256.8	5000	0.011	2.97	47.62	73594	2.32	1.17E-23
KB186-26	250	256.8	5000	0.018	2.95	28.02	55620	2.38	9.28E-23
Bossier Shale									
SHSI 6-2	250	256.2	5000	0.006	2.95	78.34	93928	2.26	2.13E-24
SHSI 1-6	250	256.7	5000	0.008	3.00	62.40	85110	2.29	3.91E-24
SCN 3-6	250	264.4	5000	0.007	2.81	71.88	86389	2.26	4.93E-24
SMY 4-2	250	266.5	5000	0.006	2.84	84.67	94584	2.24	2.43E-24
BSA1	250	254.2	5000	0.007	2.95	67.44	87135	2.28	3.64E-24
BSA2	250	258.4	5000	0.016	2.91	31.44	58378	2.36	6.97E-23
BSA3	250	260.9	5000	0.021	2.95	24.19	51614	2.40	1.58E-22
BSA4	250	258.7	5000	0.023	2.96	22.52	49863	2.41	2.00E-22
Haynesville Shale									
SBI 8-2	250	264.7	5000	0.013	2.81	38.32	62847	2.33	4.83E-23
SOM 4-4	250	262.9	5000	0.008	2.83	60.88	79848	2.28	8.41E-24
SOM 9-2	250	262.3	5000	0.008	2.87	66.97	84777	2.27	5.08E-24
HSA1	250	261.0	5000	0.025	2.88	20.36	46104	2.42	4.11E-22
HSA2	250	264.1	5000	0.021	2.87	23.72	49841	2.40	2.35E-22
HSA3	250	258.9	5000	0.017	2.96	29.67	57464	2.37	7.17E-23
HSO1	250	259.6	5000	0.008	2.93	62.31	83079	2.28	5.33E-24
HSJ2	250	264.7	5000	0.013	2.82	39.09	63544	2.33	4.43E-23
Eagle Ford Shale									
EFS1	250	273.5	5000	0.009	2.60	57.71	73614	2.28	2.17E-23
Jordan Oil Shale									
JS1	250	276.0	5000	0.013	2.83	37.67	62565	2.33	4.79E-23

JS2	250	274.4	5000	0.012	2.88	40.47	65870	2.32	3.01E-23
JS3	250	275.8	5000	0.014	2.84	37.37	62406	2.33	4.83E-23
JS4	250	272.0	5000	0.014	2.79	35.70	60204	2.34	6.82E-23
Newark Shale									
NS1	250	259.8	5000	0.006	2.87	83.47	94844	2.25	2.26E-24

Table S 6. Apparent permeabilities calculated using the fractal model for each individual sample; minimum pore size (χ_{min}), mean pore size ($\bar{\chi}$), maximum pore size (χ_{max}), porosity (Φ), fractal dimension (D_f), tortuosity (τ), straight length of the capillary tube (L_0), fractal tortuosity dimension (D_τ), present-day burial depth (D_{pd}), temperature (T) at current depth, mean pore fluid pressure ($\bar{p}$) at current depth, viscosity (μ), liquid permeability (K_L), slip factor (b), and apparent permeability (Kapp).

Sample	χ_{min}	$\bar{\chi}$	χ_{max}	**Φ**	**D_f**	**τ**	**L_0**	**D_τ**	**Fluid**	**D_{pd}**	**T**	$\bar{p}$	**μ**	**K_L**	**b**	**K_{app}**
	nm	nm	nm	-	-	-	nm	-	-	m	K	MPa	Pa.s	m^2	KPa	m^2
Opalinus Clay																
CCP01	25	35.54	2500	0.121	2.93	4.53	10143	2.73	H2	250	290.5	1.23	8.82E-06	1.78E-21	25.40	1.82E-21
CCP04	25	36.13	2500	0.111	2.92	4.89	10589	2.72	H2	250	290.5	1.23	8.82E-06	1.33E-21	25.40	1.35E-21
CCP05	25	36.44	2500	0.119	2.92	4.58	10154	2.73	H2	250	290.5	1.23	8.82E-06	1.81E-21	25.42	1.85E-21
CCP06	25	36.45	2500	0.104	2.93	5.18	10990	2.71	H2	250	290.5	1.23	8.82E-06	1.00E-21	25.37	1.02E-21
CCP07	25	35.81	2500	0.128	2.93	4.29	9784	2.74	H2	250	290.5	1.23	8.82E-06	2.34E-21	25.42	2.39E-21
CCP09	25	35.55	2500	0.109	2.93	4.97	10732	2.72	H2	250	290.5	1.23	8.82E-06	1.19E-21	25.38	1.21E-21
CCP10	25	35.54	2500	0.120	2.96	4.54	10229	2.73	H2	250	290.5	1.23	8.82E-06	1.60E-21	25.36	1.64E-21
CCP12	25	35.68	2500	0.129	2.98	4.25	9884	2.74	H2	250	290.5	1.23	8.82E-06	1.98E-21	25.33	2.03E-21
CCP14	25	34.79	2500	0.129	2.95	4.25	9793	2.74	H2	250	290.5	1.23	8.82E-06	2.24E-21	25.39	2.29E-21
Boom Clay																
BC-K4	25	37.05	2500	0.141	2.98	3.95	9410	2.75	H2	276	291.3	1.36	8.80E-06	2.86E-21	25.33	2.91E-21
BC-K10	25	36.38	2500	0.135	2.97	4.09	9590	2.75	H2	197	288.9	0.97	8.77E-06	2.53E-21	25.17	2.60E-21
BC-K11	25	39.69	2500	0.154	2.99	3.63	8954	2.76	H2	198	288.9	0.97	8.77E-06	4.00E-21	25.15	4.10E-21
BC-K2	25	38.92	2500	0.154	2.99	3.64	8965	2.76	H2	233	290.0	1.14	8.80E-06	3.97E-21	25.29	4.06E-21

BC-K9	25	36.77	2500	0.159	2.96	3.53	8683	2.77	H2	261	290.8	1.28	8.81E-06	5.37E-21	25.42	5.47E-21
Vale Shale																
VS1	25	36.88	2500	0.156	2.95	3.60	8789	2.77	CO2	2500	319.0	5.89	1.39E-05	4.93E-21	9.01	4.94E-21
VS2	25	35.56	2500	0.147	2.96	3.79	9107	2.76	CO2	2500	319.0	5.89	1.39E-05	3.76E-21	9.00	3.77E-21
VS3	25	33.86	2500	0.133	2.92	4.14	9522	2.75	CO2	2500	319.0	5.89	1.39E-05	2.93E-21	9.02	2.94E-21
Carmel Claystone																
NPS069	25	28.48	2500	0.032	2.87	15.85	20162	2.58	CO2	200	289.0	0.98	1.48E-05	1.48E-23	9.03	1.50E-23
NPS073	25	29.11	2500	0.040	2.78	12.87	17610	2.60	CO2	200	289.0	0.98	1.48E-05	4.53E-23	9.10	4.57E-23
NPS077	25	30.75	2500	0.057	2.88	9.11	15014	2.64	CO2	200	289.0	0.98	1.48E-05	1.16E-22	9.06	1.17E-22
NPS080	25	31.98	2500	0.050	2.75	10.35	15556	2.62	CO2	200	289.0	0.98	1.48E-05	1.13E-22	9.13	1.14E-22
NPS083	25	30.37	2500	0.024	2.89	21.62	23886	2.54	CO2	200	289.0	0.98	1.48E-05	4.27E-24	8.99	4.31E-24
NPS086	25	29.95	2500	0.055	2.92	9.51	15547	2.64	CO2	200	289.0	0.98	1.48E-05	8.47E-23	9.03	8.55E-23
NPS089	25	30.14	2500	0.047	2.94	10.98	16938	2.62	CO2	200	289.0	0.98	1.48E-05	4.40E-23	9.01	4.44E-23
NPS095	25	29.68	2500	0.053	2.93	9.84	15909	2.64	CO2	200	289.0	0.98	1.48E-05	7.02E-23	9.02	7.09E-23
Big Hole Carmel																
BH2CC16b	25	35.36	2500	0.033	2.86	15.38	19831	2.57	CO2	200	289.0	0.98	1.48E-05	1.62E-23	9.02	1.64E-23
Entrada Siltstone																
EPS1004	25	36.96	2500	0.047	2.67	11.11	15868	2.60	CO2	220	289.6	1.08	1.46E-05	1.09E-22	9.08	1.10E-22
EPS3049	25	33.82	2500	0.018	2.71	27.76	25954	2.50	CO2	222	289.7	1.09	1.46E-05	3.19E-24	8.98	3.22E-24
EPS3057	25	33.92	2500	0.031	2.72	16.45	19785	2.56	CO2	222	289.7	1.09	1.46E-05	2.14E-23	9.02	2.16E-23
EPS3058	25	31.39	2500	0.022	2.83	22.87	24179	2.53	CO2	222	289.7	1.09	1.46E-05	4.35E-24	8.92	4.38E-24
EPS3059	25	32.75	2500	0.033	2.65	15.40	18801	2.57	CO2	222	289.7	1.09	1.46E-05	3.47E-23	9.07	3.50E-23
EPS3061	25	30.70	2500	0.025	2.64	20.66	21886	2.54	CO2	222	289.7	1.09	1.46E-05	1.22E-23	9.06	1.23E-23
EPS3062	25	33.08	2500	0.031	2.71	16.40	19728	2.56	CO2	222	289.7	1.09	1.46E-05	2.21E-23	9.02	2.23E-23
EPS3063	25	31.07	2500	0.020	2.80	25.16	25184	2.52	CO2	222	289.7	1.09	1.46E-05	3.47E-24	8.94	3.49E-24
EPS3065	25	32.63	2500	0.033	2.64	15.58	18902	2.57	CO2	222	289.7	1.09	1.46E-05	3.37E-23	9.07	3.39E-23
EPS3066	25	32.15	2500	0.034	2.68	15.25	18842	2.57	CO2	222	289.7	1.09	1.46E-05	3.25E-23	9.05	3.28E-23

EPS3071	25	33.19	2500	0.042	2.93	12.27	17897	2.60	CO2	222	289.7	1.09	1.46E-05	3.03E-23	8.91	3.06E-23
EPS3073	25	30.27	2500	0.026	3.00	19.58	23455	2.55	CO2	222	289.7	1.09	1.46E-05	3.95E-24	8.83	3.98E-24
EPS3075	25	33.88	2500	0.031	2.70	16.65	19822	2.56	CO2	222	289.7	1.09	1.46E-05	2.18E-23	9.03	2.20E-23
EPS3076	25	33.08	2500	0.030	2.70	16.82	19940	2.56	CO2	222	289.7	1.09	1.46E-05	2.09E-23	9.03	2.11E-23
Posidonia Shale																
RWEP6	25	37.93	250	0.047	2.61	10.97	1555	2.35	CH4	2500	358.0	12.28	1.99E-05	8.35E-23	224.38	8.50E-23
RWEP10	25	36.25	250	0.045	2.62	11.53	1601	2.35	CH4	2500	358.0	12.28	1.99E-05	6.68E-23	224.19	6.80E-23
RWEP14	25	36.24	250	0.047	2.48	10.97	1516	2.36	CH4	2500	358.0	12.28	1.99E-05	1.24E-22	226.55	1.26E-22
Carboniferous Shale																
KB186-13	25	30.90	250	0.020	2.42	25.16	2322	2.25	CH4	1185	318.6	5.82	1.99E-05	5.96E-24	213.11	6.18E-24
KB186-15	25	39.05	250	0.028	2.51	18.41	2006	2.26	CH4	1187	318.6	5.83	1.99E-05	1.41E-23	211.84	1.46E-23
KB186-17	25	29.76	250	0.028	2.46	18.02	1965	2.31	CH4	1191	318.7	5.85	1.99E-05	1.98E-23	213.42	2.05E-23
KB186-19	25	31.14	250	0.022	2.49	23.37	2267	2.26	CH4	1192	318.8	5.85	1.99E-05	6.36E-24	212.16	6.59E-24
KB186-25	25	31.84	250	0.036	2.67	14.19	1809	2.34	CH4	1197	318.9	5.88	1.99E-05	2.61E-23	210.74	2.70E-23
KB186-26	25	31.84	250	0.063	2.65	8.26	1340	2.44	CH4	1197	318.9	5.88	1.99E-05	2.58E-22	212.47	2.68E-22
Bossier Shale																
SHSI 6-2	25	31.23	250	0.018	2.59	27.84	2531	2.24	CH4	3661	392.8	17.98	2.22E-05	2.43E-24	261.13	2.46E-24
SHSI 1-6	25	31.68	250	0.023	2.67	22.02	2277	2.28	CH4	3673	393.2	18.03	2.32E-05	4.72E-24	271.47	4.79E-24
SCN 3-6	25	39.44	250	0.025	2.66	20.72	2202	2.25	CH4	3746	395.4	18.39	2.34E-05	5.59E-24	274.05	5.67E-24
SMY 4-2	25	41.51	250	0.021	2.64	24.24	2378	2.21	CH4	3762	395.9	18.47	2.34E-05	3.17E-24	274.45	3.21E-24
BSA1	25	29.22	250	0.026	2.85	19.35	2227	2.32	CH4	4000	403.0	19.64	2.22E-05	4.29E-24	261.37	4.35E-24
BSA2	25	33.40	250	0.053	2.81	9.88	1540	2.40	CH4	3500	388.0	17.19	2.22E-05	6.90E-23	258.47	7.00E-23
BSA3	25	35.86	250	0.084	2.85	6.32	1209	2.48	CH4	3000	373.0	14.73	2.22E-05	3.96E-22	254.01	4.03E-22
BSA4	25	33.66	250	0.089	2.86	5.98	1174	2.50	CH4	2950	371.5	14.48	2.22E-05	4.97E-22	253.70	5.06E-22
Haynesville Shale																
SBI 8-2	25	39.75	250	0.044	2.71	11.73	1650	2.34	CH4	3766	396.0	18.49	2.34E-05	4.49E-23	275.47	4.56E-23
SOM 4-4	25	37.88	250	0.023	2.63	21.73	2243	2.25	CH4	4041	404.2	19.84	2.40E-05	5.19E-24	285.46	5.27E-24

SOM 9-2	25	37.28	250	0.027	2.77	19.09	2166	2.27	CH4	4054	404.6	19.91	2.40E-05	5.45E-24	283.85	5.53E-24
HSA1	25	36.05	250	0.102	2.77	5.29	1066	2.51	CH4	2900	370.0	14.24	2.39E-05	1.16E-21	274.23	1.19E-21
HSA2	25	39.12	250	0.091	2.77	5.90	1136	2.47	CH4	2500	358.0	12.28	2.39E-05	7.06E-22	269.19	7.21E-22
HSA3	25	33.94	250	0.052	2.86	10.07	1574	2.40	CH4	4200	409.0	20.62	2.39E-05	5.38E-23	284.62	5.46E-23
HSO1	25	34.64	250	0.029	2.82	17.46	2096	2.30	CH4	4450	416.5	21.85	2.39E-05	6.57E-24	286.08	6.66E-24
HSJ2	25	39.75	250	0.038	2.72	13.65	1791	2.31	CH4	4300	412.0	21.11	2.39E-05	2.40E-23	286.67	2.43E-23
Eagle Ford Shale																
EFS1	25	48.45	250	0.036	2.50	14.38	1760	2.26	CH4	3700	394.0	18.17	2.39E-05	3.46E-23	283.38	3.52E-23
Jordan Oil Shale																
JS1	25	50.99	250	0.063	2.67	8.31	1352	2.35	CH4	1750	335.5	8.59	0.0015	1.97E-22	5964.91	3.34E-22
JS2	25	49.45	250	0.054	2.72	9.56	1479	2.34	CH4	1750	335.5	8.59	0.0015	9.30E-23	5936.97	1.57E-22
JS3	25	50.78	250	0.057	2.68	9.14	1427	2.34	CH4	1750	335.5	8.59	0.0015	1.30E-22	5955.68	2.20E-22
JS4	25	47.00	250	0.058	2.63	9.06	1406	2.35	CH4	1750	335.5	8.59	0.0015	1.60E-22	5980.39	2.71E-22
Newark Shale																
NS1	25	34.81	250	0.019	2.57	26.79	2470	2.23	CH4	3962	401.9	19.45	2.38E-05	2.85E-24	283.18	2.89E-24

Table S 7. Effective diffusion coefficients calculated using the fractal model for all mudrocks; solute, bulk phase diffusion (D_b), minimum pore size (χ_{min}), mean pore size ($\bar{\chi}$), maximum pore size (χ_{max}), porosity (Φ), fractal dimension (D_f), tortuosity (τ), Straight length of the capillary tube (L_0), fractal tortuosity dimension (D_τ), effective diffusion coefficients (D_{eff}), and relative error.

Sample	**Solute**	**D_b**	**Porosity**	**D_f**	χ_{min}	$\bar{\chi}$	χ_{max}	**Lo**	**τ**	**Dτ**	**D_{eff}**		**Relative Error**
		m^2/s	-	-	nm	nm	nm	nm	-	-	m^2/sec		-
											Fractal	Experimental	$\lvert(D_{exp} - D_{fra})/D_{exp}\rvert$
Opalinus Clay													
CCP01	HTO	1.60E-09	0.240	2.94	2.5	10.54	5000	13393.69	2.49	2.87	6.98E-11	5.40E-11	0.29
CCP04	HTO	1.60E-09	0.210	2.93	2.5	11.13	5000	14543.18	2.78	2.86	5.53E-11	5.40E-11	0.02
CCP05	HTO	1.60E-09	0.270	2.92	2.5	11.44	5000	12315.32	2.26	2.88	9.05E-11	5.40E-11	0.68
CCP06	HTO	1.60E-09	0.200	2.93	2.5	11.45	5000	15017.86	2.90	2.85	5.04E-11	5.40E-11	0.07

CCP07	HTO	1.60E-09	0.270	2.93	2.5	10.81	5000	12352.74	2.26	2.88	8.93E-11	5.40E-11	0.65
CCP09	HTO	1.60E-09	0.210	2.94	2.5	10.55	5000	14581.86	2.78	2.86	5.47E-11	5.40E-11	0.01
CCP10	HTO	1.60E-09	0.230	2.96	2.5	10.54	5000	13871.91	2.58	2.87	6.22E-11	5.40E-11	0.15
CCP12	HTO	1.60E-09	0.240	2.98	2.5	10.68	5000	13582.71	2.49	2.87	6.52E-11	5.40E-11	0.21
CCP14	HTO	1.60E-09	0.240	2.95	2.5	9.79	5000	13456.87	2.49	2.87	6.84E-11	5.40E-11	0.27
Boom Clay													
BC-K4	HTO	1.60E-09	0.290	3.04	2.5	12.05	5000	12166.6	2.14	2.89	8.68E-11	2.50E-10	0.65
BC-K10	HTO	1.60E-09	0.320	3.08	2.5	11.38	5000	11522.93	1.98	2.90	9.91E-11	2.10E-10	0.53
BC-K11	HTO	1.60E-09	0.340	2.99	2.5	14.69	5000	10673.62	1.90	2.90	1.36E-10	1.80E-10	0.25
BC-K2	HTO	1.60E-09	0.360	2.99	2.5	13.92	5000	10212.42	1.82	2.91	1.57E-10	1.80E-10	0.13
BC-K9	HTO	1.60E-09	0.370	3.05	2.5	11.77	5000	10199.29	1.78	2.91	1.51E-10	1.60E-10	0.06
BC-K4	CH4	1.80E-09	0.290	3.04	2.5	12.05	5000	12166.6	2.14	2.89	9.76E-11	1.60E-10	0.39
BC-K10	CH4	1.80E-09	0.320	3.08	2.5	11.38	5000	11522.93	1.98	2.90	1.11E-10	1.10E-10	0.01
BC-K11	CH4	1.80E-09	0.340	2.99	2.5	14.69	5000	10673.62	1.90	2.90	1.52E-10	8.40E-11	0.81
BC-K2	CH4	1.80E-09	0.360	2.99	2.5	13.92	5000	10212.42	1.82	2.91	1.77E-10	9.70E-11	0.83
BC-K9	CH4	1.80E-09	0.370	3.05	2.5	11.77	5000	10199.29	1.78	2.91	1.70E-10	8.80E-11	0.93
Vale Shale													
VS1	CO2	1.70E-09	0.385	2.96	2.5	11.88	5000	9574.42	1.73	2.92	2.16E-10	--	--
VS2	CO2	1.70E-09	0.365	2.96	2.5	10.56	5000	10007.01	1.80	2.91	1.84E-10	--	--
VS3	CO2	1.70E-09	0.320	2.92	2.5	8.86	5000	10917.81	1.98	2.90	1.42E-10	--	--
NPS069	CO2	1.70E-09	0.044	2.73	2.5	3.48	5000	33050.42	11.68	2.73	7.34E-12	--	--
NPS073	CO2	1.70E-09	0.054	2.64	2.5	4.11	5000	29279.58	9.70	2.74	9.13E-12	--	--
NPS077	CO2	1.70E-09	0.076	2.74	2.5	5.75	5000	24839.71	6.94	2.77	1.47E-11	--	--
NPS080	CO2	1.70E-09	0.067	2.62	2.5	6.98	5000	25846.83	7.83	2.75	1.21E-11	--	--
NPS083	CO2	1.70E-09	0.026	2.85	2.5	5.37	5000	45094.45	19.81	2.67	3.89E-12	--	--
NPS086	CO2	1.70E-09	0.073	2.78	2.5	4.95	5000	25708.6	7.25	2.77	1.39E-11	--	--

NPS089	CO2	1.70E-09	0.064	2.80	2.5	5.14	5000	27785.97	8.24	2.75	1.16E-11	--	--
NPS095	CO2	1.70E-09	0.070	2.79	2.5	4.68	5000	26277.57	7.49	2.77	1.33E-11	--	--
BH2CC16b	CO2	1.70E-09	0.046	2.73	2.5	10.36	5000	32219.69	11.16	2.70	7.16E-12	--	--
EPS1004	CO2	1.70E-09	0.062	2.55	2.5	11.96	5000	26573.82	8.45	2.72	1.02E-11	--	--
EPS3049	CO2	1.70E-09	0.027	2.66	2.5	8.82	5000	41601.25	18.57	2.65	3.42E-12	--	--
EPS3057	CO2	1.70E-09	0.044	2.59	2.5	8.92	5000	32297.34	11.87	2.70	6.21E-12	--	--
EPS3058	CO2	1.70E-09	0.027	2.87	2.5	6.39	5000	44017.82	18.74	2.67	4.14E-12	--	--
EPS3059	CO2	1.70E-09	0.045	2.52	2.5	7.75	5000	31158.22	11.38	2.71	6.46E-12	--	--
EPS3061	CO2	1.70E-09	0.029	2.86	2.5	5.70	5000	42396.31	17.46	2.68	4.55E-12	--	--
EPS3062	CO2	1.70E-09	0.046	2.58	2.5	8.08	5000	31412.72	11.29	2.71	6.74E-12	--	--
EPS3063	CO2	1.70E-09	0.026	2.91	2.5	6.07	5000	45990.16	19.82	2.67	4.04E-12	--	--
EPS3065	CO2	1.70E-09	0.045	2.52	2.5	7.63	5000	31343.56	11.53	2.71	6.32E-12	--	--
EPS3066	CO2	1.70E-09	0.046	2.55	2.5	7.15	5000	31178.51	11.27	2.71	6.72E-12	--	--
EPS3071	CO2	1.70E-09	0.071	2.79	2.5	8.19	5000	26053.48	7.41	2.75	1.30E-11	--	--
EPS3073	CO2	1.70E-09	0.030	2.93	2.5	5.27	5000	42447.23	16.84	2.69	4.96E-12	--	--
EPS3075	CO2	1.70E-09	0.043	2.57	2.5	8.88	5000	32391.09	12.02	2.70	6.03E-12	--	--
EPS3076	CO2	1.70E-09	0.043	2.57	2.5	8.08	5000	32588.42	12.14	2.70	6.00E-12	--	--
Posidonia Shale													
RWEP6	CH4	1.80E-09	0.060	2.91	2.5	12.93	5000	29515.59	8.71	2.72	1.06E-11	--	--
RWEP10	CH4	1.80E-09	0.061	2.92	2.5	11.25	5000	29384.36	8.58	2.73	1.09E-11	--	--
RWEP14	CH4	1.80E-09	0.065	2.77	2.5	11.24	5000	27207.78	8.06	2.73	1.20E-11	--	--
KB186-13	CH4	1.80E-09	0.027	3.19	2.5	5.90	5000	49289.98	18.66	2.68	4.94E-12	--	--
KB186-15	CH4	1.80E-09	0.041	2.79	2.5	14.05	5000	35090.26	12.67	2.68	6.36E-12	--	--
KB186-17	CH4	1.80E-09	0.042	3.27	2.5	4.76	5000	41053.49	12.39	2.72	6.82E-12	--	--

KB186-19	CH4	1.80E-09	0.034	3.09	2.5	6.14	5000	42048.89	14.96	2.69	6.07E-12	--	--
KB186-25	CH4	1.80E-09	0.048	2.97	2.5	6.84	5000	33917.56	10.81	2.72	8.50E-12	--	--
KB186-26	CH4	1.80E-09	0.107	2.95	2.5	6.84	5000	21806	5.06	2.80	2.23E-11	--	--
Bossier Shale													
SHSI 6-2	CH4	1.80E-09	0.027	2.95	2.5	6.23	5000	45177.38	18.80	2.67	4.61E-12	--	--
SHSI 1-6	CH4	1.80E-09	0.034	3.00	2.5	6.68	5000	41036.39	15.18	2.69	5.88E-12	--	--
SCN 3-6	CH4	1.80E-09	0.049	2.81	2.5	14.44	5000	31838.22	10.52	2.69	8.15E-12	--	--
SMY 4-2	CH4	1.80E-09	0.031	2.84	2.5	16.51	5000	40589.4	16.31	2.64	4.61E-12	--	--
BSA1	CH4	1.80E-09	0.040	3.09	2.5	4.22	5000	38760.44	12.82	2.72	7.27E-12	--	--
BSA2	CH4	1.80E-09	0.079	2.91	2.5	8.40	5000	25449.25	6.69	2.76	1.53E-11	--	--
BSA3	CH4	1.80E-09	0.136	2.95	2.5	10.86	5000	19014.12	4.05	2.81	3.03E-11	--	--
BSA4	CH4	1.80E-09	0.140	2.96	2.5	8.66	5000	18791.65	3.96	2.82	3.15E-11	--	--
SBI 8-2	CH4	1.80E-09	0.062	2.81	2.5	14.75	5000	28314.32	8.48	2.72	1.09E-11	--	--
SOM 4-4	CH4	1.80E-09	0.037	2.83	2.5	12.88	5000	37245.9	13.93	2.67	5.75E-12	--	--
SOM 9-2	CH4	1.80E-09	0.051	2.87	2.5	12.28	5000	31840.61	10.20	2.70	8.68E-12	--	--
HSA1	CH4	1.80E-09	0.198	2.88	2.5	11.05	5000	14846.96	2.92	2.85	6.00E-11	--	--
HSA2	CH4	1.80E-09	0.158	2.87	2.5	14.12	5000	16999.68	3.55	2.82	4.09E-11	--	--
HSA3	CH4	1.80E-09	0.083	2.96	2.5	8.94	5000	25157.84	6.40	2.77	1.58E-11	--	--
HSO1	CH4	1.80E-09	0.044	2.93	2.5	9.64	5000	34959.26	11.76	2.70	7.49E-12	--	--
HSJ2	CH4	1.80E-09	0.061	2.82	2.5	14.75	5000	28641.04	8.64	2.72	1.06E-11	--	--
EFS1	CH4	1.80E-09	0.054	2.60	2.5	23.45	5000	29031.81	9.72	2.68	8.22E-12	--	--
JS1	CH4	1.80E-09	0.091	2.83	2.5	25.99	5000	23093.9	5.90	2.74	9.48E-12	--	--
JS2	CH4	1.80E-09	0.077	2.88	2.5	24.45	5000	25635.28	6.88	2.72	6.75E-12	--	--
JS3	CH4	1.80E-09	0.083	2.84	2.5	25.78	5000	24223.16	6.38	2.73	7.61E-12	--	--

JS4	CH4	1.80E-09	0.103	2.79	2.5	22.00	5000	21257.72	5.23	2.76	1.73E-11	--	--
Newark Shale													
NS1	CH4	1.80E-09	0.033	2.87	2.5	9.81	5000	39818.03	15.44	2.67	5.32E-12	--	--

S3.4. Pore Volume Distribution of All Mudrocks

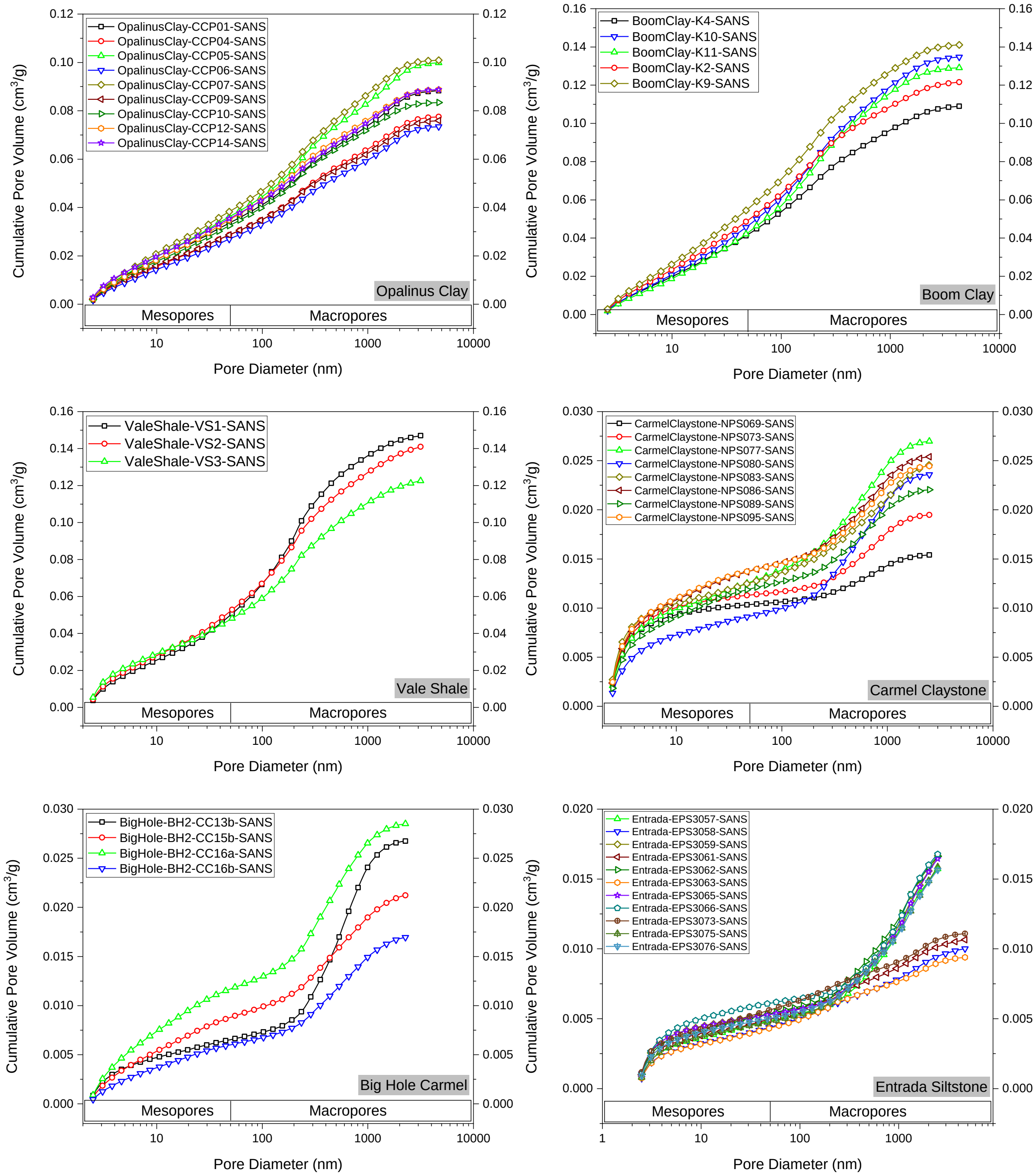

Figure S 3. Pore volume distribution of all mudrocks obtained by SANS.

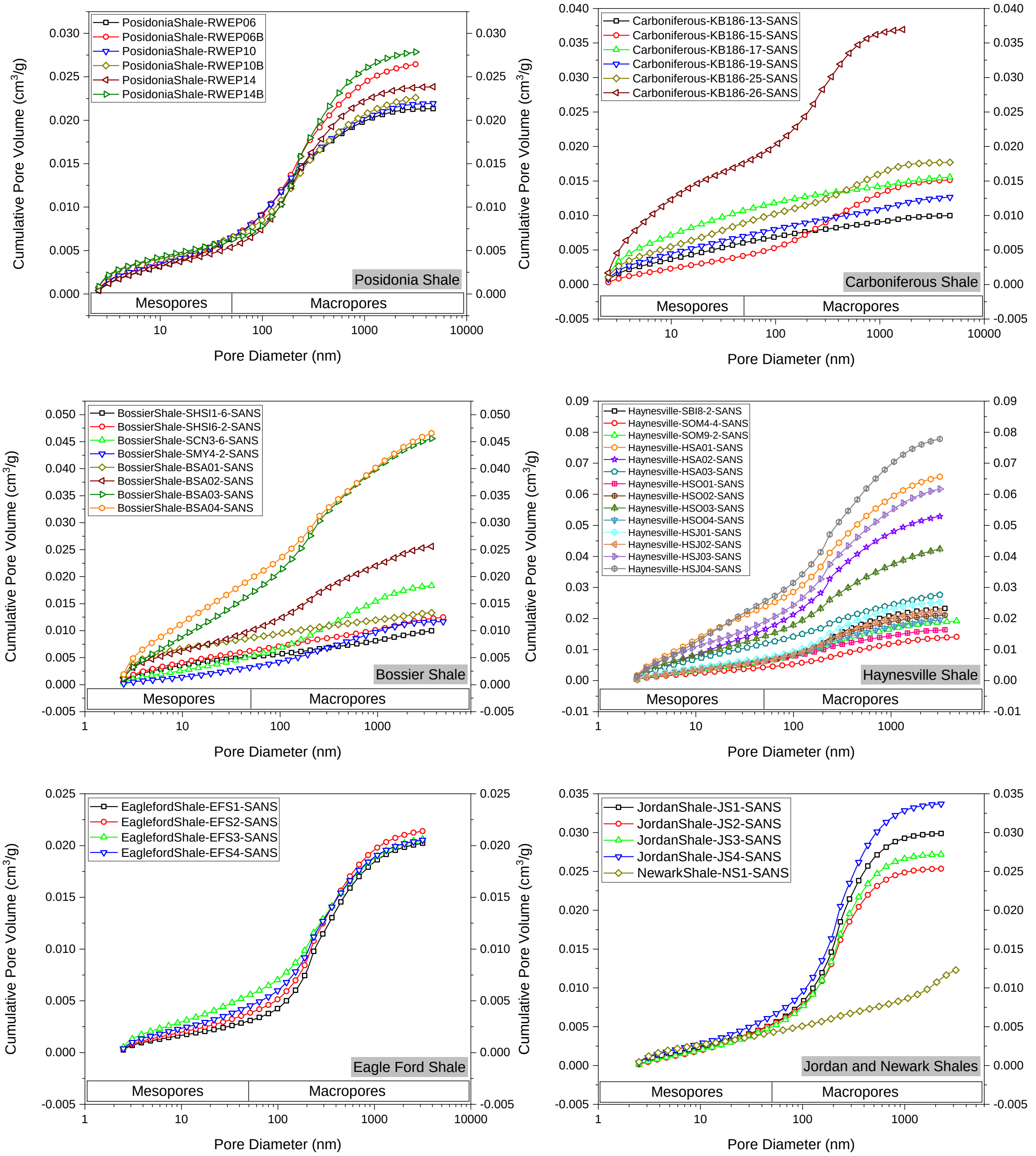

Figure S 3. (continued).

S4. Nomenclature

Alphabet Letters

A	cm^2	Beam cross sectional area
b	Pa	Slip factor
b_i	cm	Proportion by coherent scattering amplitude of the nucleus i in the component j
D; D_f	-	Fractal dimension
D_{aq}	m^2/s	Aqueous diffusion coefficient

D_{pd}	m	Present-day (current) burial depth
D_{eff}	m^2/s	Effective diffusion coefficients
D_p	-	Pore fractal dimension
D_s	-	Surface fractal dimension
D_τ	-	Tortuosity fractal dimension
d	g/cm^3	Mass density
$d\Sigma$	-	Elemental scattering cross section
$d\Omega$	-	Solid angle element
$f(r)$	$Å^{-1}$	Probability density of the pore size distribution
h	cm	Sample thickness
$I; I(Q)$	cm^{-1}	Scattering intensity
I_0	s^{-1}	Incident intensity
K_{app}	m^2	Apparent permeability
K_D	m^2	Darcy permeability
K_L	m^2	Intrinsic permeability
K_n	-	Knudsen number
$\overline{Kn}$	-	Average Knudsen number
k	$Å^{-1}$	Wave vector in the scattered direction
k_0	$Å^{-1}$	Wave vector in the straight direction
L	nm	Tortuous length of capillary tubes
L_0	nm	Straight length of capillary tubes
$M; MW$	g/mol	Atomic mass of the mixture; gas molecular weight
m	-	Slope; power-law exponent
N_A	mol^{-1}	Avogadro’s number
P	Pa	Pressure
$P(Q)$	-	Form factor
$\bar{P}_p$	Pa	Intrinsic pore fluid pressure
$\bar{p}$	Pa	Mean gas pore pressure
p_j	-	Proportion by molecular number of the component j in the mixture
Q	$Å^{-1}$	Scattering vector
$R;r$	nm	Pore radius
R_{max}	nm	Maximum pore radius
R_{min}	nm	Minimum pore radius
T	K	Temperature
$V; V_p$	cm^3	Pore volume
$\bar{V}$	cm^3	Average pore volume
VR_r	%	Vitrinite reflectance

Greek Letters

δ	nm	Mean free path
ζ	-	The exponent for the VSS model
η	-	Viscosity index
κ	-	Intermolecular collision coefficient for the VSS model
θ	-	Scattering angle
λ	Å	Wavelength
μ_g	Pa.s	Gas viscosity
ρ	g/cm^3	Mineral density
ρ^*_{matrix}	cm^{-2}	Neutron scattering length density of matrix

ρ_{pore}^{*}	cm^{-2}	Neutron scattering length density of pore
τ	-	Tortuosity
$\bar{\tau}$	-	Average tortuosity
Φ_0	cm^{-2}/s	Incident flux
φ	-	Porosity
χ	nm	Pore size or pore diameter
χ_{max}	nm	Maximum pore size
$\bar{\chi}$	nm	Mean pore size
χ_{min}	nm	Minimum pore size

Abbreviations

MATSAS	MATLAB for Small Angle Scattering
MFP	Mean Free Path
OLM	Organic Lean Mudrock
ORM	Organic Rich Mudrock
PDSP	Polydisperse Spherical Model
PSD	Pore Size Distribution
SANS	Small Angle Neutron Scattering
SLD	Scattering Length Density
SSA	Specific Surface Area
TOC	Total Organic Carbon
VSANS	Very Small Angle Neutron Scattering
VSS	Variable Soft Sphere
XRD	X-Ray Diffraction

References

Amireh, Belal S. 1997. Sedimentology and palaeogeography of the regressive-transgressive Kurnub Group (Early Cretaceous) of Jordan. *Sedimentary Geology* **112** (1): 69-88.

Bernard, Sylvain, Horsfield, Brian, Schulz, Hans-Martin et al. 2012. Geochemical evolution of organic-rich shales with increasing maturity: A STXM and TEM study of the Posidonia Shale (Lower Toarcian, northern Germany). *Marine and Petroleum Geology* **31** (1): 70-89.

Bird, G.A. 1994. *Molecular Gas Dynamics and the Direct Simulation of Gas Flows*: Clarendon Press.

Blakey, Ronald C., Havholm, Karen G., and Jones, Lawrence S. 1996. Stratigraphic analysis of eolian interactions with marine and fluvial deposits, Middle Jurassic Page Sandstone and Carmel Formation, Colorado Plateau, U.S.A. *Journal of Sedimentary Research* **66** (2): 324-342.

Bossart, Paul and Thury, Marc. 2008. Mont Terri Rock Laboratory Project, Programme 1996 to 2007 and Results, Wabern, Switzerland.

Busch, Andreas, Schweinar, Kevin, Kampman, Niko et al. 2017. Determining the porosity of mudrocks using methodological pluralism. *Geological Society, London, Special Publications* **454**.

Dawson, W. C. and Almon, W. R. 2010. Eagle Ford Shale variability: Sedimentologic influences on source and reservoir character in an unconventional resource unit. *Gulf Coast Assoc Geol Soc, Trans* **60**: 181-190.

Doebelin, Nicola and Kleeberg, Reinhard. 2015. Profex: a graphical user interface for the Rietveld refinement program BGMN. *Journal of Applied Crystallography* **48** (5): 1573-1580.

Fink, R., Amann-Hildenbrand, A., Bertier, P. et al. 2018. Pore structure, gas storage and matrix transport characteristics of lacustrine Newark shale. *Marine and Petroleum Geology* **97**: 525-539.

Gjelberg, J., Martinsen, O. J., Charnock, M. et al. 2005. The reservoir development of the Late Maastrichtian–Early Paleocene Ormen Lange gas field, Møre Basin, Mid-Norwegian Shelf. *Geological Society, London, Petroleum Geology Conference series* **6** (1): 1165-1184.

Hammes, Ursula and Frébourg, Gregory. 2012. Haynesville and Bossier mudrocks: A facies and sequence stratigraphic investigation, East Texas and Louisiana, USA. *Marine and Petroleum Geology* **31** (1): 8-26.

Jacops, E., Aertsens, M., Maes, N. et al. 2017a. Interplay of molecular size and pore network geometry on the diffusion of dissolved gases and HTO in Boom Clay. *Applied Geochemistry* **76**: 182–195.

Jacops, E., Aertsens, M., Maes, N. et al. 2017b. Interplay of molecular size and pore network geometry on the diffusion of dissolved gases and HTO in Boom Clay. *Applied Geochemistry* **76**: 182-195.

Kampman, N., Bickle, M. J., Maskell, A. et al. 2014. Drilling and sampling a natural CO2 reservoir: Implications for fluid flow and CO2-fluid–rock reactions during CO2 migration through the overburden. *Chemical Geology* **369**: 51-82.

Kampman, N., Busch, A., Bertier, P. et al. 2016. *Article*. Observational evidence confirms modelling of the long-term integrity of CO2-reservoir caprocks. *Nature Communications* **7**: 12268.

Kampman, Niko Jan Sterland. 2011. *Fluid-Rock Interactions in a Carbon Storage Site Analogue, Green River, Utah*. PhD, University of Cambridge, UK.

Klaver, Jop, Desbois, Guillaume, Littke, Ralf et al. 2015. BIB-SEM characterization of pore space morphology and distribution in postmature to overmature samples from the Haynesville and Bossier Shales. *Marine and Petroleum Geology* **59**: 451-466.

Klaver, Jop, Desbois, Guillaume, Urai, Janos L. et al. 2012. BIB-SEM study of the pore space morphology in early mature Posidonia Shale from the Hils area, Germany. *International Journal of Coal Geology* **103**: 12-25.

Littke, Ralf, Urai, Janos L., Uffmann, Anna K. et al. 2012. Reflectance of dispersed vitrinite in Palaeozoic rocks with and without cleavage: Implications for burial and thermal history modeling in the Devonian of Rursee area, northern Rhenish Massif, Germany. *International Journal of Coal Geology* **89**: 41-50.

Melnichenko, Y. B. 2015. *Small-Angle Scattering from Confined and Interfacial Fluids: Applications to Energy Storage and Environmental Science*, 329. TN, USA: Springer.

NIST. Scattering Length Density Calculator. *National Institute of Standards and Technology (NIST) Center for Neutron Research*, https://www.ncnr.nist.gov/resources/sldcalc.html.

Olsen, P. E., Kent, D. V., Cornet, B. et al. 1996. *Article*. High-resolution stratigraphy of the Newark rift basin (early Mesozoic, eastern North America). *Bulletin of the Geological Society of America* **108** (1): 40-77.

Radlinski, A.P., Ioannidis, M.A., Hinde, A.L. et al. 2002. Multiscale characterization of reservoir rock microstructure: combining small angle neutron scattering and image analysis. *Proc.*, Proceedings of 2002 International Symposium of the Society of Core Analysts (SCA2002-35), Monterey, California, Sept. 23-27.

Radlinski, Andrzej P. 2006. Small-Angle Neutron Scattering and the Microstructure of Rocks. *Reviews in Mineralogy and Geochemistry* **63** (1): 363-397.

Rezaeyan, Amirsaman, Pipich, Vitaliy, and Busch, Andreas. 2021. MATSAS: A Small Angle Scattering Computer Tool for Porous Systems. *Journal of Applied Crystallography* **54**.

Ufer, K., Stanjek, H., Roth, G. et al. 2008. QUANTITATIVE PHASE ANALYSIS OF BENTONITES BY THE RIETVELD METHOD. *Clays and Clay Minerals* **56** (2): 272-282.

Vandenberghe, Noël, Craen, Mieke De, and Wouters, Laurent. 2014. The Boom Clay Geology From sedimentation to present-day occurrence: A review, Royal Belgian Institute Of Natural Sciences, Belgium.

Vandewijngaerde, Wim, Piessens, Kris, Dusar, Michiel et al. 2016. Investigations on the shale oil and gas potential of Westphalian mudstone successions in the Campine Basin, NE Belgium (well KB174): Palaeoenvironmental and palaeogeographical controls. *Geologica Belgica* **19** (3-4): 1-30.

Zeelmaekers, E., Honty, M., Derkowski, A. et al. 2015. Qualitative and quantitative mineralogical composition of the Rupelian Boom Clay in Belgium. *Clay Minerals* **50** (2): 249-272.